bioRxiv preprint doi: https://doi.org/10.1101/370940; this version posted July 17, 2018. The copyright holder for this preprint (which was not certified by peer review) is the author/funder, who has granted bioRxiv a license to display the preprint in perpetuity. It is made available under aCC-BY 4.0 International license.

Host adaptation and convergent evolution increases antibiotic resistance without loss of virulence in a major human pathogen

Running title: Host adaptation and convergent evolution in a major human pathogen

Alicia Fajardo-Lubián[1,*], Nouri L. Ben Zakour[1], Alex Agyekum[1], Jonathan R. Iredell[1*]

[1] Centre for Infectious Diseases and Microbiology, The Westmead Institute for Medical Research, The University of Sydney and Westmead Hospital, Sydney, New South Wales, Australia.

[*] Corresponding authors.

CIDM, The Westmead Institute for Medical Research, 176 Hawkesbury Road, Westmead, NSW 2145, Australia. Fax: +61 2 8627 3099.

Email address: jonathan.iredell@sydney.edu.au (J.R. Iredell), Tel.: +61286273411

Email address: alicia.fajardolubian@sydney.edu.au (A. Fajardo-Lubian), Tel.: +612 86273415.

bioRxiv preprint doi: https://doi.org/10.1101/370940; this version posted July 17, 2018. The copyright holder for this preprint (which was not certified by peer review) is the author/funder, who has granted bioRxiv a license to display the preprint in perpetuity. It is made available under aCC-BY 4.0 International license.

Abstract

As human population density and antibiotic exposure increases, specialised bacterial subtypes have begun to emerge. Arising among species that are common commensals and infrequent pathogens, antibiotic-resistant 'high-risk clones' have evolved to better survive in the modern human. Here, we show that the major matrix porin (OmpK35) of *Klebsiella pneumoniae* is not required in the mammalian host for colonisation, pathogenesis, nor for antibiotic resistance, and that it is commonly absent in pathogenic isolates. This is found in association with, but apparently independent of, a highly specific change in the co-regulated partner porin, the osmoporin (OmpK36), which provides enhanced antibiotic resistance without significant loss of fitness in the mammalian host. These features are common in well-described 'high-risk clones' of *K. pneumoniae*, as well as in unrelated members of this species and similar adaptations are found in other members of the Enterobacteriaceae that share this lifestyle. Available sequence data indicates evolutionary convergence, with implications for the spread of lethal antibiotic-resistant pathogens in humans.

bioRxiv preprint doi: https://doi.org/10.1101/370940; this version posted July 17, 2018. The copyright holder for this preprint (which was not certified by peer review) is the author/funder, who has granted bioRxiv a license to display the preprint in perpetuity. It is made available under aCC-BY 4.0 International license.

Author summary

Klebsiella pneumoniae is a Gram-negative enterobacteria and a significant cause of human disease. It is a frequent agent of pneumonia, and systemic infections can have high mortality rates (60%). OmpK35 and OmpK36 are the major co-regulated outer membrane porins of *K. pneumoniae*. OmpK36 absence has been related to antibiotic resistance but decreased bacterial fitness and diminished virulence. A mutation that constricts the porin channel (Gly134Asp135 duplication in loop 3 of the porin, OmpK36GD) has been previously observed and suggested as a solution to the fitness cost imposed by loss of OmpK36.

In the present study we constructed isogenic mutants to verify this and test the impact of these porin changes on antimicrobial resistance, fitness and virulence. Our results show that loss of OmpK35 has no significant cost in bacterial survival in nutrient-rich environments nor in the mammalian host, consistent with a predicted role outside that niche. When directly compared with the complete loss of the partner osmoporin OmpK36, we found that isogenic OmpK36GD strains maintain high levels of antibiotic resistance and that the GD duplication significantly reduces neither gut colonisation nor pathogenicity in a pneumonia mouse model. These changes are widespread in unrelated genomes. Our data provide clear evidences that specific variations in the loop 3 of OmpK36 and the absence of OmpK35 in *K. pneumoniae* clinical isolates are examples of successful adaptation to human colonization/infection and antibiotic pressure, and are features of a fundamental evolutionary shift in this important human pathogen.

bioRxiv preprint doi: https://doi.org/10.1101/370940; this version posted July 17, 2018. The copyright holder for this preprint (which was not certified by peer review) is the author/funder, who has granted bioRxiv a license to display the preprint in perpetuity. It is made available under aCC-BY 4.0 International license.

Introduction

Host adaptation and niche specialisation is well described in bacteria. As human population density rises, commensals and pathogens among the Enterobacteriaceae are transmitted directly from human to human and increasingly exposed to antibiotics. *K. pneumoniae* is now a common cause of healthcare-associated infections and is one of the most important agents of human sepsis [1]. High morbidity and mortality is associated with acquired antibiotic resistance, most importantly by horizontal transfer of genes encoding extended-spectrum β-lactamases (ESBL) [2] and plasmid-mediated AmpC β-lactamases (pAmpC) [3]. Carbapenem antibiotics have been effective against such isolates for decades but resistance to these antibiotics is increasingly common in turn [4] and in February 2017, carbapenem resistant Enterobacteriaceae were listed as highest ('critical') research priorities by the World Health Organisation. Acquired genes encoding efficient carbapenem hydrolysing enzymes [5] typically require phenotypic augmentation by permeability reduction to be clinically relevant in the Enterobacteriaceae. Indeed, clinically significant carbapenem resistance may even be seen with the less specialised AmpC or ESBL enzymes in strains with sufficiently reduced outer membrane permeability [6, 7].

K. pneumoniae expresses two major nonspecific porins (OmpK35 and OmpK36) through which nutrients and other hydrophilic molecules such as β-lactams diffuse into the cell [8, 9]. The expression of these two major porins in *K. pneumoniae* are strongly linked with β-lactam susceptibility [6, 7] and strains lacking both porins exhibit high levels of resistance [10]. *K. pneumoniae* is commonly present in the human gut [1] but also grows in low-nutrient and low-osmolarity conditions, with decreased expression of the 'osmoporin', OmpK36, and increased expression of the 'matrix porin', OmpK35, which has the greater general permeability. In the mammalian host *in vivo*, and in nutritious media *in vitro*,

bioRxiv preprint doi: https://doi.org/10.1101/370940; this version posted July 17, 2018. The copyright holder for this preprint (which was not certified by peer review) is the author/funder, who has granted bioRxiv a license to display the preprint in perpetuity. It is made available under aCC-BY 4.0 International license.

OmpK36 is the principal general porin and the gateway for β-lactam antibiotics, these being the most frequently prescribed antibiotic class in humans and the cornerstone of therapy for serious infections.

The fitness cost of certain antibiotic resistance mutations is well described [11-14]. Significantly reduced expression of porins provides some protection from β-lactam antibiotics but may incur a considerable metabolic cost as vital nutrients are simultaneously excluded [15]. Outer membrane permeability is thus a balance between self-defence and competitive fitness [16, 17]. Global antibiotic restriction policies are founded on the premise of an inverse relationship between competitive fitness and resistance to antibiotics [18] and the expectation that antibiotic-resistant mutants will fail to successfully compete with their antibiotic-susceptible ancestors [19]. However, analysis of the principal porin relevant to infection in the mammalian host, OmpK36, revealed a key role for a transmembrane β-strand loop (loop3, L3) in the porin inner channel (‘eyelet’), which is electronegative at physiological pH. Minor changes in this region have been observed that are expected to be relatively permissive of small nutrient molecule diffusion but which may exclude more bulky anionic carbapenem and cephalosporin antibiotics [20].

Highly antibiotic-resistant *K. pneumoniae* is both a critical threat pathogen and a model of adaptation in a world with increasing human density and antibiotic exposure. The aim of this study was therefore to understand the pathogenesis and antimicrobial resistance implications of common changes in major porins that diminish membrane permeability.

bioRxiv preprint doi: https://doi.org/10.1101/370940; this version posted July 17, 2018. The copyright holder for this preprint (which was not certified by peer review) is the author/funder, who has granted bioRxiv a license to display the preprint in perpetuity. It is made available under aCC-BY 4.0 International license.

Materials and methods

Bacterial strains, plasmids, primers and growth conditions.

Bacterial strains, plasmids and primers used in this study are listed in Tables 1 and S1. Porin mutants were constructed in three antibiotic-susceptible *K. pneumoniae* strains (ATCC 13883, and clinical isolates 10.85 and 11.76 from our laboratory). Bacterial isolates were stored at -80°C in Nutrient broth (NB) with 20% glycerol and recovered on LB agar plates. Unless otherwise indicated, strains were routinely grown in Mueller-Hinton broth (MHB, BD Diagnostics, Franklin lakes, NJ, USA) or Luria-Bertani (LB, Life Technologies, Carlsbad, CA, USA). *E. coli* and *K. pneumoniae* strains carrying the chloramphenicol-resistant plasmids pKM200 and pCACtus were grown at 30°C on LB agar or in LB broth supplemented with 20 μg/ml chloramphenicol (Sigma-Aldrich, St. Louis, MO, USA). The growth of bacterial cells was determined by measuring the optical density at 600 nm (OD_{600}) in an Eppendorf Biophotometer (Eppendorf AG, Hamburg, Germany).

bioRxiv preprint doi: https://doi.org/10.1101/370940; this version posted July 17, 2018. The copyright holder for this preprint (which was not certified by peer review) is the author/funder, who has granted bioRxiv a license to display the preprint in perpetuity. It is made available under aCC-BY 4.0 International license.

Table 1 Bacterial strains used in this study

Strain	Relevant characteristic(s)[a]	Source or reference[b]
K. pneumoniae		
ATCC13883	*Klebsiella pneumoniae,* ATCC 13883	ATCC
ATCCΔOmpK35	OmpK35 deletion strain of ATCC 13883; Tet^r	TS
ATCCOmpK36GD	OmpK36 L3 GD strain of ATCC 13883	TS
ATCCΔOmpK36	OmpK36 deletion strain of ATCC 13883; Km^r	TS
ATCCΔOmpK35OmpK36GD	OmpK35 deletion strain with OmpK36 L3 GD; Tet^r	TS
ATCCΔOmpK35ΔOmpK36	OmpK35 and OmpK36 deletion strain of ATCC 13883; Tet^r:Km^r	TS
10.85	Wild-type *Klebsiella pneumoniae,* clinical isolate	[21]
10.85ΔOmpK35	OmpK35 deletion strain of 10.85; Tet^r	TS
10.85OmpK36GD	OmpK36 L3 GD strain of ATCC 13883	TS
10.85ΔOmpK36	OmpK36 deletion strain of ATCC 13883; Km^r	TS
10.85ΔOmpK35OmpK36GD	OmpK35 deletion strain with OmpK36 L3 GD; Tet^r	TS
10.85ΔOmpK35ΔOmpK36	OmpK35 and OmpK36 deletion strain of ATCC 13883; Tet^r:Km^r	TS
11.76	Wild-type *Klebsiella pneumoniae,* clinical isolate	[21]
11.76ΔOmpK35	OmpK35 deletion strain of ATCC 13883; Tet^r	TS
11.76OmpK36GD	OmpK36 L3 GD strain of ATCC 13883	TS
11.76ΔOmpK36	OmpK36 deletion strain of ATCC 13883; Km^r	TS
11.76ΔOmpK35OmpK36GD	OmpK35 deletion strain with OmpK36 L3 GD; Tet^r	TS
11.76ΔOmpK35ΔOmpK36	OmpK35 and OmpK36 deletion strain of ATCC 13883; Tet^r:Km^r	TS
JIE1333	OmpK36 L3 GD *K. pneumoniae,* clinical isolate	[21]
JIE1334	OmpK36 L3 GD *K. pneumoniae,* clinical isolate	[21]
JIE1335	OmpK36 L3 GD *K. pneumoniae,* clinical isolate	[21]
JIE1348	OmpK36 L3 GD *K. pneumoniae,* clinical isolate	[21]
JIE1383	OmpK36 L3 GD *K. pneumoniae,* clinical isolate	[21]
JIE1462	OmpK36 L3 GD *K. pneumoniae,* clinical isolate	[21]
JIE1474	OmpK36 L3 GD *K. pneumoniae,* clinical isolate	[21]
JIE1482	OmpK36 L3 GD *K. pneumoniae,* clinical isolate	[21]
JIE2038	OmpK36 L3 GD *K. pneumoniae,* clinical isolate	[21]
JIE2055	OmpK36 L3 GD *K. pneumoniae,* clinical isolate	[21]
JIE2218	OmpK36 L3 GD *K. pneumoniae,* clinical isolate	[21]
JIE4101	OmpK36 L3 TD *K. pneumoniae,* clinical isolate	WH
JIE4111	OmpK36 L3 TD *K. pneumoniae,* clinical isolate	WH
JIE4212	OmpK36 L3 GD *K. pneumoniae,* clinical isolate	WH
JIE4609	OmpK36 L3 TD *K. pneumoniae,* clinical isolate	WH
JIE4656	OmpK36 L3 TD *K. pneumoniae,* clinical isolate	WH
JIE4735	OmpK36 L3 TD *K. pneumoniae,* clinical isolate	WH

bioRxiv preprint doi: https://doi.org/10.1101/370940; this version posted July 17, 2018. The copyright holder for this preprint (which was not certified by peer review) is the author/funder, who has granted bioRxiv a license to display the preprint in perpetuity. It is made available under aCC-BY 4.0 International license.

E. coli		
DH5α	*hsdR17 recAl*; high efficiency transformation strain	[22]
S17 λpir	λpir lysogen of S17 (Tp^r Sm^r *thi pro* Δ*hsdR hsdM*$^+$ *recA* RP4::2-Tc::Mu-*km*::Tn7)	[23]

[a]L3 GD: Gly+Asp duplication in loop 3, ATCC, American Type Culture collection, Tet^r; Tetracycline resistant, Km^r; Kanamycin resistant

[b]TS, This study. WH, Westmead Hospital.

117

118 **Construction of porin mutants**

119 Chemical transformation, conjugations and electroporation were carried out using
120 standard protocols. Platinum pfx DNA polymerase (Invitrogen, USA) was used to amplify
121 blunt-ended PCR products. All PCR products were purified (PureLink Quick PCR
122 Purification Kit; Invitrogen, USA). PCR and sequencing was used to confirm all constructs.
123 Genomic DNA extractions were performed using a DNeasy Blood and Tissue kit (Qiagen,
124 Valencia, CA, USA) and plasmid DNA using a PureLink Quick Plasmid Miniprep kit (Life
125 Technologies, Carlsbad, CA, USA) or a HiSpeed Plasmid Midi Kit (Qiagen, Valencia, CA,
126 USA).

127 Porin deletions mutants of *K. pneumoniae* ATCC 13883, 10.85 and 11.76 were
128 created by introduction of *tetA* (tetracycline-resistance) or *aphA-3* (kanamycin-resistance)
129 into unique sites in *ompK35* and *ompK36* (HincII and StuI, respectively) which had been
130 previously cloned into pGEM-T easy (Promega, Madison, WI, USA). The disrupted porin
131 genes were then cloned into pCACtus suicide temperature-sensitive vector (pJIAF-7 to
132 PJIAF-12) to replace the respective chromosomal genes by homologous recombination [24].
133 Confirmation of correct single-copy chromosomal mutations were finally verified by PCR
134 (Table S1).

135 OmpK36GD mutants were obtained by amplification of OmpK36 from each parental
136 strain using K36GD1 / K36GD2 and K36GD3 / K36GD4 primers (Table S1). The amplicon,

bioRxiv preprint doi: https://doi.org/10.1101/370940; this version posted July 17, 2018. The copyright holder for this preprint (which was not certified by peer review) is the author/funder, who has granted bioRxiv a license to display the preprint in perpetuity. It is made available under aCC-BY 4.0 International license.

137 containing a GD duplication in L3, was cloned first in pGEM-T easy and after digestion with
138 *Sph1* and *Sac1* (New England Biolabs, MA, USA) was introduced into pCACtus. The
139 pCACtus-based construct (pJIAF-13 to pJIAF-18) was transformed into S17λpir and
140 conjugated into *K. pneumoniae* ΔOmpK36 (kanamycin-resistance mutant) where the
141 interrupted gene was replaced by OmpK36 porin with GD duplication in L3 by homologous
142 recombination. Mutants were selected by loss of kanamycin resistance and confirmed by
143 PCR and sequencing.

144 Double mutants (ΔOmpK35ΔOmpK36 and ΔOmpK35OmpK36GD) were constructed
145 using lambda Red-mediated recombineering as described previously [25, 26], with some
146 modifications. A tetracycline cassette flanked by OmpK35 deletion (~2.5 kb in size) was
147 PCR amplified from an OmpK35 deletion mutant (ΔOmpK35; tetracycline resistant-
148 previously obtained) using primers ompK35X-F and ompK35X-R (Table S1) and PCR
149 products were purified. Red Helper plasmid pKM200 was electroporated into ΔOmpK36 or
150 OmpK36GD single mutants. *ompK35:tetA* fragments were electroporated into ΔOmpK36 or
151 OmpK36GD clones carrying pKM200. Bacteria were grown at 30°C for 2 h with agitation
152 (225 rpm) followed by overnight incubation at 37°C. Different dilutions of the electroporated
153 cells were spread on LB agar plates containing 10 μg/ml tetracycline to select for
154 transformants at 37°C. The correct structure was confirmed by sequencing of PCR amplicons
155 (primers ompK35F1 and ompK35R2, Table S1).

156 **Antimicrobial susceptibility tests**

157 Susceptibilities to cefazolin (CFZ, Sigma-Aldrich, St. Louis, MO, USA), cephalothin
158 (CEF, Sigma-Aldrich, St. Louis, MO, USA), cefoxitin (FOX, Sigma-Aldrich, St. Louis, MO,
159 USA), cefuroxime (CXM, Sigma-Aldrich, St. Louis, MO, USA), cefotaxime (CTX, A.G.
160 Scientific, Inc., San Diego, CA, USA), ceftazidime (CAZ, Sigma-Aldrich, St. Louis, MO,

bioRxiv preprint doi: https://doi.org/10.1101/370940; this version posted July 17, 2018. The copyright holder for this preprint (which was not certified by peer review) is the author/funder, who has granted bioRxiv a license to display the preprint in perpetuity. It is made available under aCC-BY 4.0 International license.

USA), ertapenem (ETP, Sigma-Aldrich, St. Louis, MO, USA), imipenem (IPM, Sigma-Aldrich, St. Louis, MO, USA), meropenem (MEM, A.G Scientific, Inc, San Diego, CA, USA) and ampicillin (MEM, A.G Scientific, Inc, San Diego, CA, USA) were performed by broth microdilution in cation-adjusted Mueller-Hinton (MH) broth (Becton Dickinson) with inocula of 5 x 10^5 CFU/ml in accordance with CLSI MO7-A9 recommendations [27]. All MICs were determined in triplicate at least on three separate occasions to obtain at least 9 discrete data points and compared with EUCAST and CLSI clinical breakpoints for all antibiotics [28, 29]. *E. coli* (ATCC25922) and *Pseudomonas aeruginosa* (ATCC27853) were included in each experiment as quality controls.

Transfer of resistance genes

The filter mating method [30] was used to transfer plasmids from clinical isolates carrying $bla_{\text{CTX-M-15}}$, (pJIE143) [31] $bla_{\text{IMP-4}}$ (pEl1573) [32] and $bla_{\text{KPC-2}}$ (pJIE2543-1) [33] to *K. pneumoniae* ATCC 13883 and porin mutants (ΔOmpK35, ΔOmpK36, OmpK36GD, ΔOmpK35ΔOmpK36 and ΔOmpK35OmpK36GD). The presence of resistance genes in transconjugants was confirmed by PCR [33-35] and the presence of plasmids of the expected size confirmed by S1 nuclease pulsed-field gel electrophoresis (Promega, Madison, WI, USA) [36, 37].

Outer membrane porin investigation

Isolates were grown overnight in MHB. Bacteria were disrupted by sonication and outer membrane porins (OMPs) isolated with sarcosyl (Sigma-Aldrich, St. Louis, MO, USA), as previously described [21, 38]. Samples were boiled, analyzed by sodium dodecyl sulfate-polyacrylamide gel electrophoresis (SDS-PAGE) (12% separating gels), and stained with Imperial protein stain (Thermo Scientific, Rockford, IL, USA), following the manufacturer's instructions. *K. pneumoniae* ATCC 13883, which produces both porins (OmpK35 and

bioRxiv preprint doi: https://doi.org/10.1101/370940; this version posted July 17, 2018. The copyright holder for this preprint (which was not certified by peer review) is the author/funder, who has granted bioRxiv a license to display the preprint in perpetuity. It is made available under aCC-BY 4.0 International license.

185 OmpK36) was used as a control [39]. Colour prestained protein standard, broad range (11-
186 245 KDa) (New England Biolabs, MA, USA) was used as size marker.

187 **Real-time reverse transcription-PCR**

188 The expression levels of the different porins were measured by real-time RT-PCR.
189 Cells were harvested in logarithmic phase at an OD_{600} of 0.5-0.6. Total RNA was isolated
190 using RNeasy system (Qiagen). RNA was treated with DNase (TURBO DNA-*free* Kit,
191 Ambion). cDNA was synthesized by high-capacity cDNA reverse transcriptase kit (Applied
192 Biosystems). One microgram of the initially isolated RNA was used in each reverse
193 transcription reaction. cDNA was diluted 1:10 and 2 µl were used for the real-time reaction.
194 Three biological replicates, each with three technical replicates, were used in each of the
195 assays. The relative levels of expression were calculated using the threshold cycle ($2^{-\Delta\Delta CT}$)
196 method [40]. The expression of *rpoD* was used to normalize the results. The primers used are
197 listed in Table S1.

198 **Determination of growth rate**

199 Growth rates were determined as previously described [41]. Overnight broth cultures
200 were diluted 1:1000. Six aliquots of 200 µl per dilution were transferred into 96-well
201 microtiter plates (Corning Incorporated, Durham, NC, USA). Samples were incubated at
202 37°C and shaken before measurement of OD_{600} in a Vmax Kinetic microplate reader
203 (Molecular Devices, Sunnyvale, CA, USA). Growth rates and generation times were
204 calculated on OD_{600} values between 0.02-0.09. The relative growth rate was calculated by
205 dividing the generation time of each mutant by the generation time of the parental strain (*K.*
206 *pneumoniae* ATCC 13883, 10.85 or 11.76) which was included in every experiment.
207 Experiments were performed in sextuplicate in three independent cultures on three different
208 occasions. Results are expressed as means ± standard errors of the means.

bioRxiv preprint doi: https://doi.org/10.1101/370940; this version posted July 17, 2018. The copyright holder for this preprint (which was not certified by peer review) is the author/funder, who has granted bioRxiv a license to display the preprint in perpetuity. It is made available under aCC-BY 4.0 International license.

209 ***In vitro* competition experiment**

210 Competition experiments were carried out as described previously [42]. Viable cell
211 counts were obtained by plating every 24 h on antibiotic-free LB agar and on LB agar
212 supplemented with antibiotic (kanamycin 20 μg/ml or tetracycline 10 μg/ml) to distinguish
213 between mutants and wild-type cells. PCR (with pairs K36GD4 / K36GD11 or K36GD12 /
214 K36GD13 primers, Table S1) was performed for the calculation of the competition results
215 between the parental strain and OmpK36GD mutant (in this particular experiments, bacteria
216 were diluted in fresh media every 24h and PCR on 100 viable colonies of each replicate was
217 performed every 48h). All experiments were carried out in triplicate with three independent
218 cultures. Mean values of three independent experiments ± standard deviation were plotted.

219 **Mouse model of gastrointestinal tract colonization (GI) and competition experiments.**

220 Five to six week-old female BALB/c mice (Animal Resources Centre (ARC), Sydney,
221 Australia) were used for GI colonization [43-45] and competition experiments. Mice were
222 caged in groups of three and had unrestricted access to food and drinking water. Faecal
223 samples were collected and screened for the presence of indigenous *K. pneumoniae* before
224 inoculation. For the colonization study, three mice were inoculated with the parental strain or
225 a porin mutant (1 x 10^{10} CFU / mouse), suspended in 20% (w/v) sucrose. For individual
226 colonization, ampicillin was added to drinking water on day 4 (0.5 g / L) after an inoculation
227 [46]. For the competition experiment, equal volumes of the parental strain and each mutant or
228 equal volume of different mutants (1x 10^{10} CFU / mouse) were mixed and suspended in 20%
229 (w/v) sucrose. Colonization was maintained with ampicillin 0.5 g / L throughout the
230 experiment [47-49]. Faeces samples were collected every second day, emulsified in 0.9%
231 NaCl and appropriate serial dilutions plated on MacConkey-inositol-carbenicillin agar, which
232 selectively recovers for *K. pneumoniae* [50].

bioRxiv preprint doi: https://doi.org/10.1101/370940; this version posted July 17, 2018. The copyright holder for this preprint (which was not certified by peer review) is the author/funder, who has granted bioRxiv a license to display the preprint in perpetuity. It is made available under aCC-BY 4.0 International license.

Mouse model of virulence: intranasal infection.

Five-six week-old female BALB/c mice [Animal Resources Centre (ARC), Sydney, Australia] used in the inhalation (pneumonia) model [51-53] were exposed to ATCC 13883 and 10.85 and their isogenic ΔOmpK35OmpK36GD mutants. Overnight bacterial cultures were harvested, washed and resuspended at 10^9 CFU in 20 µl of saline and inoculated into the nasal passages. A control group of mice was inoculated with saline. Following infection, survival studies were performed (10 mice per strain). Organ (lung and spleen) and blood infection burdens were also assessed at various points throughout the infection period, by plating out blood and homogenised tissue onto LB agar, and counting CFU (5 mice per strain, per time point).

Structure modelling of OmpK36 variants

Tri-dimensional structural models of ATCC13883 OmpK36 and its mutated variant OmpK36GD were computed with ProMod3 Version 1.1.0 on the SWISS-MODEL online server [54] using the target–template alignment method. The best scoring model used as a template was 5nupA (93.84% sequence identity, with a QMEAN equal to -2.29 and -2.14, respectively for both sequences). For comparison purposes, models were also computed using the second best OmpK36 structure available in PDB (1osmA). All predicted models were evaluated using MolProbity [55, 56] and Verify3D [57, 58], with Ramachandran plots generated by MolProbity indicating for all computed models that at least >98% of residues were in allowed regions. Predicted structures were displayed by PyMol software (version 2.1.1) [59].

Additionally, the specific impact of di-nucleotide insertions was also investigated by altering the OmpK6 structure under PDB accession 5nupA, adding either the di-nucleotide

bioRxiv preprint doi: https://doi.org/10.1101/370940; this version posted July 17, 2018. The copyright holder for this preprint (which was not certified by peer review) is the author/funder, who has granted bioRxiv a license to display the preprint in perpetuity. It is made available under aCC-BY 4.0 International license.

GD-, TD- or SD-, after position G113 and modeling the resulting variant sequences in the same manner as mentioned above.

Genome sequencing and comparative analysis

Genomic DNA was extracted from 2 ml overnight cultures using the DNeasy Blood and Tissue kit (Qiagen). Paired-end multiplex libraries were prepared using the Illumina Nextera kit in accordance with the manufacturer's instructions. Whole genome sequencing was performed on Illumina NextSeq 500 (150bp paired-end) at the Australian Genome Research Facility (AGRF). Raw sequence reads are available on NCBI under Bioproject accession number PRJNA430457. Reads were quality-checked, trimmed and assembled using the Nullarbor pipeline v.1.20 (available at: https://github.com/tseemann/nullarbor), as previously described [60], but with the exception of the assembly step which was performed using Shovill (available at: https://github.com/tseemann/shovill), a genome assembler pipeline wrapped around SPAdes v.3.9.0 [61] which includes post-assembly correction. Assemblies were also reordered against reference strain *K. pneumoniae* 30660/NJST258_1 (accession number CP006923) using progressive Mauve v.2.4.0 [62] prior to annotation with Prokka [63] and screened for antibiotic resistance genes using Abricate v.0.6 (available at: https://github.com/tseemann/abricate).

Population analysis

To investigate the significance of *ompK35* and *ompK36* mutations in a wider population, we collected a total of 1,557 draft and complete *K. pneumoniae* genomes publicly available in Genbank (Feb 2017, Table S2). Sequences were typed using Kleborate v0.1.0 [64] to identify MLST (Table S3) and minimum spanning trees were generated using Bionumerics v.7.60. Presence and absence of porins were assessed in the pangenome using Roary v3.6.0 [65] with default parameters and mutations in loop 3 (L3) identified using BLAST. The 2,253,033 nt core genes alignment predicted by Roary was used to build a

bioRxiv preprint doi: https://doi.org/10.1101/370940; this version posted July 17, 2018. The copyright holder for this preprint (which was not certified by peer review) is the author/funder, who has granted bioRxiv a license to display the preprint in perpetuity. It is made available under aCC-BY 4.0 International license.

maximum-likelihood tree using IQ-TREE v1.6.1 [66], with a GTR+G+I nucleotide substitution model and branch supports assessed with ultrafast bootstrap approximation (1000 replicates). Trees were visualized alongside contextual information with Phandango [67].

Statistical analysis was performed using Chi-tests and extended mosaic plots in R, to determine associations between ST, porin defects and other relevant population metrics such as country of origin, year and source of isolation. Relevant R scripts were also made available at https://github.com/nbenzakour/Klebsiella_antibiotics_paper.

Ethics Statement

For gastrointestinal gut colonization, animal experiments were approved by the Western Sydney Local Health District Animal Ethics Committee (AEC Protocol no. 4205.06.13).

For intranasal infection, animal experiments were approved by the Western Sydney Local Health District Animal Ethics Committee (AEC Protocol no. 4275.06.17).

All research and animal care procedures were in accordance with the "Australian Code of Practice for the Care and Use of Animals for Scientific Purposes", 8th Edition (2013) (National Health and Medical Research Council, Australian Government).

Results

Outer membrane porins and resistance to beta-lactam antibiotics

Minimal inhibitory concentrations for commonly used carbapenems (Ertapenem and Meropenem), third-generation cephalosporins (Ceftazidime, Cefotaxime and Ceftriaxone),

bioRxiv preprint doi: https://doi.org/10.1101/370940; this version posted July 17, 2018. The copyright holder for this preprint (which was not certified by peer review) is the author/funder, who has granted bioRxiv a license to display the preprint in perpetuity. It is made available under aCC-BY 4.0 International license.

cephamycins (also called 'second generation cephalosporins', Cefoxitin and Cefuroxime), first generation cephalosporins (Cephalothin and Cefazolin), and the semi-synthetic penicillin Ampicillin were determined in three *K. pneumoniae* strains and their isogenic porin mutants, with representative results in Table 2 (for complete results, see Table S4). The SHV enzyme characteristically expressed by *K. pneumoniae* hydrolyses ampicillin very effectively, providing high MICs to ampicillin [68-71], but does not provide clinically important resistance to cephalosporins or carbapenems in the setting of normal membrane permeability.

Loss of OmpK36 (ΔK36 in Tables 2 and S4) is associated with a minor increase in MIC for carbapenems and cephalosporins (Tables 2 and S4), with a lesser impact from OmpK36GD mutations, consistent with an important role for OmpK36 in the nutritious growth media (MHB) normally used for standardised MIC determinations (Tables 2 and S4).

Table 2 Antibiotic MICs *K. pneumoniae* ATCC 13883 and porin mutants

	Antibiotics, MIC (mg/L)[a]					
Strain	**ETP**	**MEM**	**CAZ**	**CTX**	**FOX[b]**	**CEF[b]**
ATCC 13883	0.015	0.03	0.5	0.06	8	8
ΔK35	0.03	0.06	1	0.125	16	8-16
ΔK36	**0.0625**	0.06	1	**0.25**	16-32	**32**
K36GD	0.03-0.06	0.03-0.06	1	0.25	16-32	16-32
ΔK35ΔK36	**1**	**0.125-0.25**	1	**0.5**	**64**	**64**
ΔK35K36GD	**0.25**	0.06	1	**0.5**	**64**	**32-64**

MIC. Minimal Inhibitory Concentration. ETP, Ertapenem (S ≤ 0.5, R > 1). MEM, Meropenem (S ≤ 2, R > 8). CAZ, Ceftazidime (S ≤ 1, R > 4). CTX, Cefotaxime (S ≤ 1, R > 2). FOX, Cefoxitin (S ≤ 8, R ≥ 32). CEF, Cephalothin (S ≤ 8, R ≥ 32)..
[a]Boldface numbers indicate at least 4-fold increase in MIC. Underlined MICs are non-susceptible according to EUCAST [72] or, for FOX and CEF[b] only, CLSI [73] breakpoints.

OmpK35 loss (ΔK35 in Tables 2 and S4) has little impact alone but further increases MICs for most antibiotics in the presence of OmpK36 lesions (e.g. ΔK35ΔK36 and ΔK35ΔK36GD). In addition to ertapenem non-susceptibility, ΔOmpK35ΔOmpK36 and ΔOmpK35OmpK36GD strains are clinically resistant to first (e.g. cephalothin, CEF) and second generation cephalosporins/ cephamycins (e.g. cefoxitin, FOX) (Tables 2 and S4).

bioRxiv preprint doi: https://doi.org/10.1101/370940; this version posted July 17, 2018. The copyright holder for this preprint (which was not certified by peer review) is the author/funder, who has granted bioRxiv a license to display the preprint in perpetuity. It is made available under aCC-BY 4.0 International license.

Naturally occurring plasmids from other *K. pneumoniae* strains encoding a common ESBL ($bla_{CTX\text{-}M\text{-}15}$) [31], a metallo-carbapenemase ($bla_{IMP\text{-}4}$) [32] and a serine-carbapenemase ($bla_{KPC\text{-}2}$) [33] were transferred into ATCC 13883 and its isogenic mutants by conjugation, with transfer verified by PCR (Table S1) and S1/PFGE (Fig. S1). Even the common ESBL CTX-M-15 confers reduced susceptibility to ETP in the presence of an OmpK36 deletion or inner channel mutation (GD duplication), especially if accompanied by an OmpK35 defect (Table 3). Expression of the specialised carbapenemases IMP and KPC from their naturally occurring plasmids resulted in greatly increased carbapenem MICs (Table 3), with the double porin mutants being highly resistant to all carbapenems tested.

Table 3 Carbapenem MICs against ATCC 13883 and porin mutants with $bla_{CTX\text{-}M\text{-}15}$, $bla_{IMP\text{-}4}$ or bla_{KPC}

	MIC (mg/L)								
	CTX-M-15			**IMP-4**			**KPC**		
Strain	ETP	MEM	IPM	ETP	MEM	IPM	ETP	MEM	IPM
ATCC 13883	0.25	0.125	1	8	8	4	16	8	8
ΔK35	0.5	0.125	1	8	8	4	32	**32**	16
ΔK36	**1**	0.25	1	8	8	4	32	**32**	**32**
K36GD	**1**	0.25	1	8	8	4	32	16	16
ΔK35ΔK36	**8**	**2**	1	**64**	**32**	**64**	**128**	**128**	**128**
ΔK35K36GD	**4**	**1**	1	**32**	**32**	**16**	**128**	**128**	**64**

MIC. Minimal Inhibitory Concentration. ETP, Ertapenem (S ≤ 0.5, R > 1). MEM, Meropenem (S ≤ 2, R > 8). IPM, Imipenem (S ≤ 2, R > 8).
[a]Boldface numbers indicate at least 4-fold increase between the MICs of the parental strain (*K. pneumoniae* ATCC 13883) and the porin mutants. The underlined numbers mean intermediate or resistant based on EUCAST breakpoints [72].

Altered expression of other common porins in ΔOmpK35, ΔOmpK36, and OmpK36GD.

Other porins may compensate for the loss of major outer membrane porins in *K. pneumoniae* [74-77]. Expression of *ompK35*, *ompK36*, *ompK37*, *phoE*, *ompK26* and *lamB* was measured in isogenic porin mutants of ATCC 13883 and 10.85 *K. pneumoniae* strains, in

bioRxiv preprint doi: https://doi.org/10.1101/370940; this version posted July 17, 2018. The copyright holder for this preprint (which was not certified by peer review) is the author/funder, who has granted bioRxiv a license to display the preprint in perpetuity. It is made available under aCC-BY 4.0 International license.

conditions in which either OmpK35 or OmpK36 are ordinarily expressed (Fig 1. Table S5). Neither the introduction of a GD duplication into the OmpK36 inner channel (OmpK36GD) nor the loss of OmpK35 (ΔOmpK35 and ΔOmpK35OmpK36GD) affected expression of OmpK36 in MH broth. Loss of OmpK36, however, was associated with increased OmpK35 expression in MH broth, in which OmpK36, but not OmpK35, is ordinarily expressed. Loss of both of these major porins (ΔOmpK35ΔOmpK36) resulted in increased expression of *phoE* and *lamB*. (Fig 1. Table S5).

Relative fitness costs of major porin lesions

Exponential phase growth in MH broth was not greatly affected unless both major porins were absent (ΔOmpK35ΔOmpK36, Table S6) but competition experiments clearly illustrate the importance of OmpK36 (Figs 2 and S2). The ability of ΔOmpK35 strains to directly compete against their intact isogenic parents in MH broth was little affected over 7 days growth (Figs S2A1, S2A3 and S2A4) but OmpK36GD strains are clearly much more able than ΔOmpK36 strains to compete with their isogenic parent strains (Figs 2A1 and 2A3). For ATCC 13883, at day 3, the OmpK36GD population was still 40% of the total combined population (Fig. 2A1), while ΔOmpK36 fell to 20% in the same period (Fig S2B1). This difference was more marked in the presence of an OmpK35 lesion, but ΔOmpK35OmpK36GD populations were still clearly more able than ΔOmpK35ΔOmpK36 to compete with the intact parent strain (Figs 2B1, 2B3 versus Figs S2C1 and S2C3). Directly competing OmpK36GD with ΔOmpK36 (and ΔOmpK35OmpK36GD with ΔOmpK35ΔOmpK36) further illustrates the competitive advantage, with OmpK36GD strains quickly displacing isogenic ΔOmpK36 strains in MH broth (Figs 2C1 and 2D1). In fact, the introduction of an OmpK36GD mutation had no detectable cost at all in *K. pneumoniae* 10.85 (Figs 2A3 and 2B3), with ΔOmpK35OmpK36GD competing very successfully against the

bioRxiv preprint doi: https://doi.org/10.1101/370940; this version posted July 17, 2018. The copyright holder for this preprint (which was not certified by peer review) is the author/funder, who has granted bioRxiv a license to display the preprint in perpetuity. It is made available under aCC-BY 4.0 International license.

isogenic parent 10.85 (Fig 2B3: 37±4% and 26±15% of the total population represented by ΔOmpK35OmpK36GD on days 6 and 7 respectively)

Mouse gut colonizing studies yielded similar results (Figs 2A2 to 2D2 and S2A2 to S2C2). Mice were confirmed not to include indigenous *K. pneumoniae* on arrival [50], and stable colonisation at ~10^9 CFU/g faeces was achieved (Fig S3). OmpK35 deficient mutants (ΔOmpK35) were not significantly disadvantaged (Fig S2A2) and OmpK36GD strains strongly outperformed OmpK36 strains in competition with their isogenic parents (Figs 2A2 and S2B2). Similarly, direct i*n vivo* competition confirmed a clear fitness advantage of OmpK36GD over ΔOmpK36 (Figs 2C2 and 2D2).

Pathogenicity is attenuated in ΔOmpK36 but not OmpK36GD or ΔOmpK35 strains

We confirmed the loss of virulence previously ascribed to loss of OmpK36 [78, 79] in a mouse pneumonia model [51-53] and, importantly, showed no difference in lethality between a wild type strain and its isogenic mutant ΔOmpK35/OmpK36GD (Fig 3). Intranasal inoculation of mice showed that these mutations had no significant impact on virulence, with equivalent mortality curves (Figs 3A1 and 3A2) and similar viable counts developing in lung, blood and spleen over the course of infection in isogenic pairs derived from both the ATCC strain and the clinical isolate 10.85 (Figs 3B to 3D).

Structural impacts of OmpK36 loop L3 mutations

Two crystal structures of native OmpK36 available in the Protein Data Bank under accession number 5nup (2.9 Å, Xray) and 1osm (3.2 Å, Xray) were evaluated as template for structural modelling of OmpK36 and OmpK36GD from ATCC 13883, with targets and templates sharing around 93% nucleotide sequence identity. While Ramachandran plots analysis for all predicted models show at least 98% of residues in allowed regions, other metrics such as QMEAN and Molprobity score are marginally better for ATCC13883

bioRxiv preprint doi: https://doi.org/10.1101/370940; this version posted July 17, 2018. The copyright holder for this preprint (which was not certified by peer review) is the author/funder, who has granted bioRxiv a license to display the preprint in perpetuity. It is made available under aCC-BY 4.0 International license.

393 OmpK36 and OmpK36GD models based on the 5nup structure (Fig. 4, Table S7). Although
394 several differences can be observed in the final alignment (Fig 4D), the most prominent
395 differences between the original structure (Fig. 4A) and the ATCC13883 OmpK36 model lie
396 within the loop L6, which can be seen in yellow, slightly obstructing the outmost channel of
397 the porin (Fig. 4B). More strinking is the impact of single di-nucleotide -GD insertion with in
398 loop L3, which is expected to constrict even more the porin channel (Fig. 4C) and is likely
399 responsible for the difference of phenotype between the 2 variants.

400 **OmpK35 loss and convergent evolution of OmpK36GD**

401 The successful antibiotic resistance, colonisation and pathogenicity phenotypes of
402 ΔOmpK35OmpK36GD strains should be reflected in their representation among strains
403 causing human infection. Of 165 unique *K. pneumoniae ompK36* sequences in GenBank,
404 16% varied from the consensus L3 inner channel motif (PEFGGD). Most common was the
405 GD duplication (PEFGGD**GD**, in 14 of 26 OmpK36 L3 variants identified), along with 6
406 additional variants: PEFGGD**D**, PEFGGD**SD**, PEFGGD**TD**, PEFGGD**TYD**, PEFGGD**TYG**
407 and PEFGGD**TYGSD** (Fig. S4). Inspection of their corresponding nucleotide sequences
408 suggests that these variants originated from various combinations of short in-frame
409 duplications, combined with additional point mutations in rare cases (Fig. S5).

410 To investigate OmpK36 among clinical isolates without specialised carbapenemases,
411 we specifically analysed L3 variation in all such *K. pneumoniae* isolates with an Ertapenem
412 MIC > 1 in our local clinical collection (Table 1) by PCR and sequencing (Table S1). Of
413 (n=51), 17 strains (33 %) were identified: all revealed either the previously described GD or
414 TD mutation in the L3 loop of *ompK36* on sequencing and these encoded up to 6 distinct
415 beta-lactamases. These isolates were genetically diverse but belonged to major epidemic
416 clones found elsewhere in the world: *i.e.* ST14, ST16, ST101, ST147, with as many as 6

bioRxiv preprint doi: https://doi.org/10.1101/370940; this version posted July 17, 2018. The copyright holder for this preprint (which was not certified by peer review) is the author/funder, who has granted bioRxiv a license to display the preprint in perpetuity. It is made available under aCC-BY 4.0 International license.

417 distinct *ompK35* mutations, all of which introduced disrupting frame-shifts and all of which
418 were relatively lineage-specific (Fig S6).

419 Finally, all *K. pneumoniae* (complete and draft) genomes available from Genbank, *i.e.*
420 1,557 entries (as of February 2017) were examined: the two common (GD and TD) variants
421 are shown in a minimum spanning tree built using MLST profiles (Fig. 5) to be distributed
422 across the whole spectrum of diversity of *K. pneumoniae*, including in most major epidemic
423 clones, *e.g.* ST258 and its derivative ST512, ST11, ST101, ST147, ST14 and ST37.

424 A maximum likelihood phylogeny using a 2,253,033 bp core genome alignment of all
425 1,557 genomes was computed to contextualize variations in *ompK36* and *ompK35,* with
426 metadata relative to the population (year, source, geographical regions of isolation, as well as
427 major beta-lactamases genes) (Fig. 6). Those genes most relevant to a carbapenem resistance
428 phenotype are shown, and the expected clustering of some of these is as expected (e.g.
429 $bla_{\text{CTX-M-15}}$ with $_{\text{OXA-1}}$ and $_{\text{TEM-1b}}$). Major associations with other genes not affected by porin
430 changes are not shown (e.g. aminoglycoside resistance due to 16S methylase genes that are
431 common companions of bla_{NDM}, other class I integron cassettes from the array in which
432 $bla_{\text{IMP-4}}$ is found, etc). The predominance of *ompK36* variations in L3 compared to its loss or
433 disruption is evident at a glance, as is the common loss or disruption of *ompK35* in unrelated
434 strains. There is no obvious relationship between OmpK36 L3 variations and the presence of
435 bla_{KPC} but there is strong clustering of these variations in certain types (ST 258, 512 etc).

436 We attempted to take sampling bias into consideration by adjusting for the
437 distribution of samples according to metrics such as ST, country, and year (Fig S7). As
438 expected for a gene so clearly linked to fitness and virulence, *ompK36* is highly conserved
439 across the population (present in 1,499 out of 1,577), independent of ST (Chisq = 207.51, df
440 = 227, p-value = 0.8188), while *ompK35* (evidently dispensable in the host) is disrupted in

bioRxiv preprint doi: https://doi.org/10.1101/370940; this version posted July 17, 2018. The copyright holder for this preprint (which was not certified by peer review) is the author/funder, who has granted bioRxiv a license to display the preprint in perpetuity. It is made available under aCC-BY 4.0 International license.

nearly a third of all strains (Fig. 6), and particularly within the major epidemic clone ST258 (Chisq = 603.7, df = 227, p-value = 5.748e-36). Three-way comparison of the presence/absence of *ompK35*, mutations in *ompK36*, and ST (considering only those STs harbouring *ompK36* GD/TD variants) shows that i) some STs tend to have both *ompK36* and *ompK35* intact (mainly ST15, ST16, ST17); ii) others tend to have intact *ompK36* with disrupted *ompK35* (ST101, ST129, ST258); and iii) some STs tend to have *ompK36* (GD/TD) variants combined with disrupted *ompK35* (ST11, ST14, ST147, ST258 and ST37) (Fig. S8). Associations between presence/absence of OmpK35, an extra aspartate in OmpK36 loop 3 and other metrics such as year or country of isolation may be confounded by over-representation of certain categories (USA, years 2011 and 2014) and we were unable to identify a definite temporal or geographical signal (Fig. S9 and S10).

Finally, we looked at associations between the number of resistance genes and porin defects in major STs, and found that the presence of *ompK36* GD/TD variants did not correlate with a higher number of resistance genes (with the exception of OmpK36GD in ST14). In fact, successful clones such as ST258 and ST11 harbouring OmpK36GD encoded significantly less resistance genes (p<0.001, Wilcoxon test) (Fig. S11).

Discussion

β-lactam antibiotics are among the most commonly prescribed for severe infections [80, 81] and the emergence of β-lactam resistance in *K. pneumoniae* has become a global health threat [82, 83]. In general, *E. coli* and *K. pneumoniae* carrying transmissible β-lactam resistance genes have predictable and normally distributed β-lactam MICs [21] but carbapenem MICs in *K. pneumonia*e are bimodally distributed with higher MICs correlating

bioRxiv preprint doi: https://doi.org/10.1101/370940; this version posted July 17, 2018. The copyright holder for this preprint (which was not certified by peer review) is the author/funder, who has granted bioRxiv a license to display the preprint in perpetuity. It is made available under aCC-BY 4.0 International license.

463 with OmpK36 defects [21]. OmpK36 loss or mutation is not uncommonly reported in highly
464 resistant clinical isolates producing KPC, ESBL or AmpC β-lactamases [20, 84, 85].

465 Diffusion of β-lactam antibiotics through non-specific porins such as OmpK35 and
466 OmpK36 is dependent on size, charge and hydrophobicity [86, 87], with bulky negatively
467 charged compounds diffusing at a lower rate than small zwitterions of the same molecular
468 weight [88]. OmpK35 is much less expressed in high osmolarity nutrient-rich conditions than
469 OmpK36, which has the narrower porin channel of the two (Fig S12) [9] and large negatively
470 charged β-lactams such as third-generation cephalosporins and carbapenems diffuse more
471 efficiently through OmpK35 than OmpK36 [78, 89]. Here we confirm the significantly
472 increased MICs, commonly attributed to mutations in these two major porins [10, 90, 91], in
473 three *K. pneumoniae* strains (the widely-published ATCC strain 13883 and two locally
474 isolated clinical strains (Tables 2 and S4); and unequivocally identify the primary role of
475 OmpK36 in carbapenem resistance.

476 Comparable MIC changes in single (OmpK36GD and ΔOmpK36) and double
477 (ΔOmpK35OmpK36GD and ΔOmpK35ΔOmpK36) mutants indicate that duplication of a
478 glycine aspartate (GD) pair in a critical position in the porin eyelet region (loop 3) is almost
479 as effective as a complete deletion of the porin in excluding large anionic antibiotics. Both
480 single and double porin mutants were susceptible to extended-spectrum cephalosporins
481 (cefotaxime and ceftazidime) in the absence of acquired hydrolysing enzymes, demonstrating
482 the impotence of the naturally occurring chromosomal SHV [68-70] against these compounds
483 [90].

484 Differences relating to porin permeability in *K pneumoniae* are most striking and
485 important in the presence of acquired carbapenemases and it is clear that these permeability
486 changes greatly enhance the associated resistance phenotypes. The common Ambler Class A

bioRxiv preprint doi: https://doi.org/10.1101/370940; this version posted July 17, 2018. The copyright holder for this preprint (which was not certified by peer review) is the author/funder, who has granted bioRxiv a license to display the preprint in perpetuity. It is made available under aCC-BY 4.0 International license.

serine protease KPC-2 and Class B metalloenzyme IMP-4 expressed from their natural plasmids produce only borderline resistance against meropenem and the smaller zwitterionic imipenem in the presence of the 'wild type' OmpK36 osmoporin (Table 3) but MICs that exceed therapeutic tissue levels [92, 93] are the rule in strains of the commonly occurring ΔOmpK35OmpK36GD genotype.

We also show here that the OmpK35 matrix porin has little or no relevance *in vivo* or in test conditions that reliably predict antibiotic efficacy in the clinic (MICs and competitive fitness in Mueller-Hinton broth). Consistent with this, a high percentage of clinical isolates whose genomes have been lodged with GenBank appear to have lost their ability to express OmpK35 altogether (Fig 6). Increased production of the larger channel OmpK35 is expected under low-temperature, low-osmolarity and low nutrient conditions (Fig S12). These favour survival outside the mammalian host and we show that ΔOmpK35 strains fail to compete successfully with their isogenic parents in nutrient-limited conditions (Fig. S13). We confirm that OmpK35 is not naturally expressed at significant levels in optimal growth conditions nor in the mammalian host, as previously described [76, 78] and competition experiments, the most sensitive and direct measures of comparative fitness, evince no discernible disadvantage from the loss of OmpK35 *in vivo,* as expected [19, 94].

Loss of OmpK36 trades off nutrient influx for antibiotic resistance [41, 78] and we show that these more resistant bacteria cannot compete successfully with the antibiotic-susceptible populations from which they arise once antibiotic selection ceases to operate (Fig S2). Double porin mutants (ΔOmpK35ΔOmpK36) are the most antibiotic-resistant (Tables 2 and S4) but this resistance comes at the cost of a 10% relative growth reduction in nutritious media (Table S6). We show that loss of OmpK36, the main porin normally expressed *in vivo*, is responsible for most of this fitness cost (Figs 2 and S2). The less permeable phosphoporin

bioRxiv preprint doi: https://doi.org/10.1101/370940; this version posted July 17, 2018. The copyright holder for this preprint (which was not certified by peer review) is the author/funder, who has granted bioRxiv a license to display the preprint in perpetuity. It is made available under aCC-BY 4.0 International license.

PhoE and maltodextrin channel LamB are most important in the usual compensatory response when OmpK35 is not available but are not very efficient substitutes (Fig 1 and Table S5). Defects in these porins have been implicated in carbapenem resistance in association with only an AmpC-type enzyme [41, 74, 77, 95] but the fitness cost may be too high for long-term success as such strains are rarely described. By contrast, ΔOmpK35OmpK36GD mutants exhibit little disadvantage compared to isogenic parents with both porins intact, *in vivo* or in optimal growth conditions *in vitro* (Fig 2, Table S6). Expression of OmpK36 is unaffected (Fig 1 and Table S5) as is that of other porins such as OmpK35 (Fig 1 and Table S5), presumably because OmpK36 'rescue' is not required.

The precise loop 3 variation in OmpK36 is evidently a convergent evolutionary process, as a range of different variants occur within genetically distant *K. pneumoniae* populations, all having in common the presentation of an extra negatively charged aspartate (D) residue that significantly constricts the inner channel (Figure 4). The most common solution is the extra glycine and aspartate (PEFGGD to PEFGGDGD in the critical region) which we recreated in isogenic mutants for our experiments. The next most frequent, an extra TD (rather than GD), is similarly likely to spontaneously arise (Fig S5) but is much less common, including in STs in which both GD and TD are found (Figs 5 and 6), implying a less optimal conformation. A recent survey of nearly 500 ertapenem-resistant *Klebsiellae* lacking specialised carbapenemases [96] supports our own finding of the extra aspartate in that position, most commonly as a GD pair, with TD and SD much less often, and other variants being quite rare (Fig. S14). We found no examples of a similarly acidic (glutamate) residue naturally occurring in this position, perhaps reflecting the fact that even simple sequence changes (here, GAY to GAR) add an additional step to a simple duplication event, or the fact that glutamate's extra carbon makes it slightly less compact than an aspartate in this position.

bioRxiv preprint doi: https://doi.org/10.1101/370940; this version posted July 17, 2018. The copyright holder for this preprint (which was not certified by peer review) is the author/funder, who has granted bioRxiv a license to display the preprint in perpetuity. It is made available under aCC-BY 4.0 International license.

Other Enterobacteria face the same challenge of excluding bulky anionic carbapenem antibiotics in order to survive high concentrations, even in the presence of a specialist carbapenemase. High level antimicrobial resistance has been ascribed to similar variations in L3 of OmpK36 homologues in *Enterobacter aerogenes*, *Escherichia coli* and *Neisseria gonorrhoeae* (Fig S15) [97-101]. In comparison with their *E. coli* homologues (OmpF and OmpC), OmpK35 and OmpK36 permit greater diffusion of β-lactams [102]. Specifically, OmpK35 appears to be highly permeable to third-generation cephalosporins such as cefotaxime due to its particular L3 domain, which is also seen in Omp35 in *E. aerogenes* but not in other species, and has been proposed as an explanation for the high proportion of *K. pneumoniae* clinical isolates that lack this porin [102, 103]. Our findings of increased MICs in OmpK35 mutants are consistent with those of others [102] but we show here that the more permeable OmpK35 is not important in the mammalian host. Rather, the much less permeable OmpK36 (equivalent to *E coli* OmpC) [102] is the bottleneck for large anionic antibiotics.

The term 'high risk clone' [104, 105] is given to host-adapted/ pathogenic strains that dominate the epidemiology of (antibiotic resistant) infections, presumably because they are more transmissible, more pathogenic and/or more tolerant of host-associated stresses (including antibiotics). Here, we see a range of unrelated clonal groups already identifiable as high-risk clones that are dispensing with the OmpK35 porin (Fig 6). The minimal antibiotic resistance advantage in nutritious media is only evident with carbapenems and is unlikely to arise in the presence of an existing OmpK36 loss mutation because the fitness cost is substantial. The loss of OmpK35 through low-level carbapenem exposure in environmental conditions is possible [106] but also has a marked fitness cost and the exposure to carbapenems in the environment is expected to be limited, as they are a still a minority class

bioRxiv preprint doi: https://doi.org/10.1101/370940; this version posted July 17, 2018. The copyright holder for this preprint (which was not certified by peer review) is the author/funder, who has granted bioRxiv a license to display the preprint in perpetuity. It is made available under aCC-BY 4.0 International license.

560 of prescribed antibiotics and are not yet as common in environmental waters as the
561 sulfonamides, quinolones, macrolides, tetracyclines and other beta-lactams [107].

562 A recent review of antibiotic resistance in *Klebsiella* pointed out that "The exact role
563 of porins in antimicrobial resistance is difficult to determine because other mechanisms…are
564 commonly present..." [108]. We suggest that host-adaptation in *K. pneumoniae* is widespread
565 and that many *K. pneumoniae* have dispensed with the OmpK35 matrix porin required for an
566 environmental life cycle. Under a major stress (as antibiotic pressure or high concentrations
567 of bile salts in the intestinal lumen), bacteria try to adapt to the new environment [109]. It has
568 been described that for *E. coli*, toxic agents as antibiotics and bile acids diffuse better through
569 the larger OmpF channel (homolog of OmpK35) than the narrower OmpC (equivalent to
570 OmpK36 in *K. pneumoniae*) [110]. At the same time, high osmolarity, high temperature, low
571 pH and anaerobiosis (typical conditions in gut environment) induce the production of
572 OmpK36 but inhibit the expression of *ompK35* [111] [112] [113]. Interestingly, *E. coli*
573 mutants with reduced permeability (decreased *ompF* and increased *ompC* mRNA and protein
574 levels compared with parental strain) can be easily recovered from intestinal gut of germ-free
575 mice after few days of colonization [114]. Convergent evolution upon a highly specific
576 variation in the inner channel of the osmoporin OmpK36 efficiently solves the problem of
577 carbapenem resistance at no cost to colonising ability, competitiveness or pathogenicity and
578 can be expected to be an increasingly common feature of host-adapted 'high-risk clones'.

579 There are three direct and immediate implications. Firstly, efforts to control the spread
580 of such strains will be facilitated to some extent by the loss of environmental hardiness
581 resulting from OmpK35 deletion, and should shift slightly more toward managing
582 interpersonal transmission. Secondly, *K. pneumoniae* can be expected to become more
583 antibiotic resistant overall and organisms expressing currently circulating plasmid-borne
584 carbapenemases will more commonly be untreatable with carbapenem antibiotics (e.g. ST258

bioRxiv preprint doi: https://doi.org/10.1101/370940; this version posted July 17, 2018. The copyright holder for this preprint (which was not certified by peer review) is the author/funder, who has granted bioRxiv a license to display the preprint in perpetuity. It is made available under aCC-BY 4.0 International license.

585 strains with *bla*$_{KPC}$); the second (higher MIC) peak in the bimodal distribution of carbapenem
586 MICs in *K. pneumoniae* populations will become more prominent. Finally, the mobile
587 carbapenemase gene pool can be expected to flourish in the protected niche provided by host-
588 adapted *K. pneumoniae* populations under strong carbapenem selection pressure in human
589 hosts, thereby increasing the general availability of highly transmissible carbapenem
590 resistance plasmids among host-adapted pathogens in the *Enterobacteriaceae*.

bioRxiv preprint doi: https://doi.org/10.1101/370940; this version posted July 17, 2018. The copyright holder for this preprint (which was not certified by peer review) is the author/funder, who has granted bioRxiv a license to display the preprint in perpetuity. It is made available under aCC-BY 4.0 International license.

Figures

Figure 1: Real-time RT-PCR in *K. pneumoniae* ATCC 13883 and 10.85 porin mutants. The expression of *rpoD* was used to normalize the results. The levels of expression of each mutant are shown relative to the wild type strain ATCC 13883 or 10.85.

Figure 2: *In vitro* and *in vivo* competition experiments in *K. pneumoniae* ATCC 13883 and 10.85 OmpK36GD porin mutants. The relative fitness of OmpK36GD porin mutants in comparison with parental strain (ATCC 13883 or 10.85) or versus ΔOmpK36 mutant was performed by competition experiments in co-cultures and expressed as a percentage of the mutant or wild type cells versus total population at each time point. *In vitro* growth conditions, MH broth, 37ºC. Panels 1 and 3 represent *in vitro* competition experiments for ATCC 13383 and 10.85, respectively. Panels in row 2 show *in vivo* competition experiments for ATCC 13383. For *in vivo* competition experiments, the values for each mouse are represented individually. Violet diamond, ATCC 13883 or 10.85 wild type strains. Green square, OmpK36GD mutant. Pink circle, ΔOmpK35OmpK36GD mutant. Red square, ΔOmpK36 mutant. Blue circle, ΔOmpK35ΔOmpK36 mutant.

Figure 3: Lung infection experiments in *K. pneumoniae* ATCC 13883 and 10.85 and their isogenic porin mutants ΔOpmK35/OmpK36GD. Survival curves after intranasal infection are represented in panels A1 (for ATCC 13883) and A2 (for 10.85). Organ burden after 24, 48 or 72h is represented in panels B1 to D1 for ATCC 13883 and B2 to D2 for 10.85. Violet diamond, ATCC 13883 or 10.85 wild type strains. Pink circle, ΔOmpK35OmpK36GD mutant.

bioRxiv preprint doi: https://doi.org/10.1101/370940; this version posted July 17, 2018. The copyright holder for this preprint (which was not certified by peer review) is the author/funder, who has granted bioRxiv a license to display the preprint in perpetuity. It is made available under aCC-BY 4.0 International license.

Figure 4: Channel restriction of OmpK36 variants. Comparison of the reference OmpK36 structure under PDB accession 5nupA (A) against predicted structural models of OmpK36 (B) and OmpK36GD mutant (C) from ATCC 13883, showing progressive restriction of the porin channel. The conformation visualised in panel B, in particular the loop 6 in yellow, which can be seen partially obstructing the channel, is not associated with a carbapenem resistance phenotype, contrary to the GD mutant shown in panel C. Panel D consists of the multiple alignment of the 3 corresponding sequences, along with a representation of the predicted secondary structures designated as follows; B for barrel, T for turn, and L for loop. Single peptide is not shown in 5nupA sequence (Panel D).

Figure 5: Minimum spanning tree of 1,557 *K. pneumoniae* strains based on their MLST profile. Each circle corresponds to a distinct ST, with its size being proportional to the number of strains of that particular ST (for scale, ST258 contains 552 isolates). Within an ST, the proportion of strains harbouring either a GD or TD insertion in the loop L3 of *ompK36* is shown as a sector coloured in red and pink, respectively. STs carrying these mutations are also circled in grey.

Figure 6: Maximum likelihood tree of 1,557 *K. pneumoniae* strains. A phylogenetic tree was built using a 2,253,033 bp long core alignment. Contextual information relative the collection was visualized using Phandango and includes ST (of which the major ones are indicated on the tree); GD or TD insertion in the loop L3 of *ompK36*, in black and red, respectively; presence or absence of *ompK36*, in orange and purple, respectively; presence or absence of *ompK35*, in orange and purple, respectively. Additional metadata include year of isolation, in a gradient from purple to yellow; source and geographical region of isolation in a rainbow gradient; and presence of major beta-lactamases (bla) alleles identified, in dark blue.

bioRxiv preprint doi: https://doi.org/10.1101/370940; this version posted July 17, 2018. The copyright holder for this preprint (which was not certified by peer review) is the author/funder, who has granted bioRxiv a license to display the preprint in perpetuity. It is made available under aCC-BY 4.0 International license.

References

1. **Podschun R, Ullmann U. *Klebsiella* spp. as nosocomial pathogens: epidemiology, taxonomy, typing methods, and pathogenicity factors. Clinical microbiology reviews. 1998;11(4):589-603.**

2. **Canton R, Coque TM. The CTX-M β-lactamase pandemic. Current opinion in microbiology. 2006;9(5):466-75.**

3. **Jacoby GA. AmpC β-lactamases. Clinical microbiology reviews. 2009;22(1):161-82.**

4. **Nordmann P, Dortet L, Poirel L. Carbapenem resistance in *Enterobacteriaceae*: here is the storm! Trends in molecular medicine. 2012;18(5):263-72.**

5. **Nordmann P, Naas T, Poirel L. Global spread of carbapenemase-producing *Enterobacteriaceae*. Emerging infectious diseases. 2011;17(10):1791-8.**

6. **Padilla E, Alonso D, Domenech-Sanchez A, Gomez C, Perez JL, Alberti S, et al. Effect of porins and plasmid-mediated AmpC β-lactamases on the efficacy of β-lactams in rat pneumonia caused by *Klebsiella pneumoniae*. Antimicrobial agents and chemotherapy. 2006;50(6):2258-60.**

bioRxiv preprint doi: https://doi.org/10.1101/370940; this version posted July 17, 2018. The copyright holder for this preprint (which was not certified by peer review) is the author/funder, who has granted bioRxiv a license to display the preprint in perpetuity. It is made available under aCC-BY 4.0 International license.

651 **7. Agyekum A, Fajardo-Lubian A, Ai X, Ginn AN, Zong Z, Guo X, et al.**
652 **Predictability of phenotype in relation to common β-lactam resistance mechanisms in**
653 ***Escherichia coli* and *Klebsiella pneumoniae*. Journal of clinical microbiology.**
654 **2016;54(5):1243-50.**

655 **8. Alberti S, Rodriquez-Quinones F, Schirmer T, Rummel G, Tomas JM,**
656 **Rosenbusch JP, et al. A porin from *Klebsiella pneumoniae*: sequence homology, three-**
657 **dimensional model, and complement binding. Infection and immunity. 1995;63(3):903-**
658 **10.**

659 **9. Hernández-Allés S, Albertí S, Alvarez D, Doménech-Sánchez A, Martínez-**
660 **Martínez L, Gil J, et al. Porin expression in clinical isolates of *Klebsiella pneumoniae*.**
661 **Microbiology. 1999;145:673-9.**

662 **10. Domenech-Sánchez A, Pascual A, Suarez AI, Alvarez D, Benedí VJ, Martínez-**
663 **Martínez L. Activity of nine antimicrobial agents against clinical isolates of *Klebsiella***
664 ***pneumoniae* producing extended-spectrum β-lactamases and deficient or not in porins.**
665 **The Journal of antimicrobial chemotherapy. 2000;46(5):858-9.**

666 **11. Andersson DI, Levin BR. The biological cost of antibiotic resistance. Current**
667 **opinion in microbiology. 1999;2(5):489-93.**

668 **12. Guo B, Abdelraouf K, Ledesma KR, Nikolaou M, Tam VH. Predicting bacterial**
669 **fitness cost associated with drug resistance. The Journal of antimicrobial chemotherapy.**
670 **2012;67(4):928-32.**

bioRxiv preprint doi: https://doi.org/10.1101/370940; this version posted July 17, 2018. The copyright holder for this preprint (which was not certified by peer review) is the author/funder, who has granted bioRxiv a license to display the preprint in perpetuity. It is made available under aCC-BY 4.0 International license.

671 **13. Marcusson LL, Frimodt-Møller N, Hughes D. Interplay in the selection of**
672 **fluoroquinolone resistance and bacterial fitness. PLoS Pathog. 2009;5(8):e1000541.**

673 **14. Choi MJ, Ko KS. Loss of hypermucoviscosity and increased fitness cost in**
674 **colistin-resistant *Klebsiella pneumoniae* sequence type 23 strains. Antimicrobial agents**
675 **and chemotherapy. 2015;59(11):6763-73.**

676 **15. Pagès JM, James CE, Winterhalter M. The porin and the permeating antibiotic:**
677 **a selective diffusion barrier in Gram-negative bacteria. Nature reviews Microbiology.**
678 **2008;6(12):893-903.**

679 **16. King T, Ishihama A, Kori A, Ferenci T. A regulatory trade-off as a source of**
680 **strain variation in the species *Escherichia coli*. Journal of bacteriology.**
681 **2004;186(17):5614-20.**

682 **17. Ferenci T. Maintaining a healthy SPANC balance through regulatory and**
683 **mutational adaptation. Molecular microbiology. 2005;57(1):1-8.**

684 **18. Ferenci T, Phan K. How porin heterogeneity and trade-offs affect the antibiotic**
685 **susceptibility of Gram-negative bacteria. Genes (Basel). 2015;6(4):1113-24.**

686 **19. Andersson DI, Hughes D. Antibiotic resistance and its cost: is it possible to**
687 **reverse resistance? Nature reviews Microbiology. 2010;8(4):260-71.**

bioRxiv preprint doi: https://doi.org/10.1101/370940; this version posted July 17, 2018. The copyright holder for this preprint (which was not certified by peer review) is the author/funder, who has granted bioRxiv a license to display the preprint in perpetuity. It is made available under aCC-BY 4.0 International license.

688 **20. Crowley B, Benedi VJ, Domenech-Sanchez A. Expression of SHV-2 β-lactamase**
689 **and of reduced amounts of OmpK36 porin in *Klebsiella pneumoniae* results in increased**
690 **resistance to cephalosporins and carbapenems. Antimicrobial agents and**
691 **chemotherapy. 2002;46(11):3679-82.**

692 **21. Agyekum A, Fajardo-Lubi A, Xiaoman A, Ginn AN, Zong Z, Guo X, et al.**
693 **Predictability of phenotype in relation to common beta-lactam resistance mechanisms in**
694 ***Escherichia coli* and *Klebsiella pneumoniae*. Journal of clinical microbiology. 2016.**

695 **22. Woodcock DM, Crowther PJ, Doherty J, Jefferson S, DeCruz E, Noyer-Weidner**
696 **M, et al. Quantitative evaluation of *Escherichia coli* host strains for tolerance to cytosine**
697 **methylation in plasmid and phage recombinants. Nucleic acids research.**
698 **1989;17(9):3469-78.**

699 **23. Crepin S, Harel J, Dozois CM. Chromosomal complementation using Tn7**
700 **transposon vectors in *Enterobacteriaceae*. Applied and environmental microbiology.**
701 **2012;78(17):6001-8.**

702 **24. Ogunniyi AD, Kotlarski I, Morona R, Manning PA. Role of SefA subunit protein**
703 **of SEF14 fimbriae in the pathogenesis of *Salmonella enterica* serovar Enteritidis.**
704 **Infection and immunity. 1997;65(2):708-17.**

705 **25. Datsenko KA, Wanner BL. One-step inactivation of chromosomal genes in**
706 ***Escherichia coli* K-12 using PCR products. Proc Natl Acad Sci U S A. 2000;97(12):6640-**
707 **5.**

bioRxiv preprint doi: https://doi.org/10.1101/370940; this version posted July 17, 2018. The copyright holder for this preprint (which was not certified by peer review) is the author/funder, who has granted bioRxiv a license to display the preprint in perpetuity. It is made available under aCC-BY 4.0 International license.

708 **26. Murphy KC, Campellone KG. Lambda Red-mediated recombinogenic**
709 **engineering of enterohemorrhagic and enteropathogenic *E. coli*. BMC Mol Biol.**
710 **2003;4:11.**

711 **27. CLSI. Methods for dilution antimicrobial susceptibility tests for bacteria that**
712 **grow aerobically. 9th edition ed: Clinical Laboratory Standards Institute, Wayne, PA;**
713 **2012.**

714 **28. EUCAST. Breakpoint tables for the interpretation of MICs and zone diameters:**
715 **European Committee on Antimicrobial Susceptibility Testing, Växjö, Sweden; 2015.**

716 **29. CLSI. Performance standards for antimicrobial susceptibility testing; Twenty-**
717 **fourth informational supplement2014.**

718 **30. Valenzuela JK, Thomas L, Partridge SR, van der Reijden T, Dijkshoorn L,**
719 **Iredell J. Horizontal gene transfer in a polyclonal outbreak of carbapenem-resistant**
720 ***Acinetobacter baumannii*. Journal of clinical microbiology. 2007;45(2):453-60.**

721 **31. Partridge SR, Ellem JA, Tetu SG, Zong Z, Paulsen IT, Iredell JR. Complete**
722 **sequence of pJIE143, a pir-type plasmid carrying IS*Ecp1*-*bla*$_{\text{CTX-M-15}}$ from an**
723 ***Escherichia coli* ST131 isolate. Antimicrobial agents and chemotherapy.**
724 **2011;55(12):5933-5.**

bioRxiv preprint doi: https://doi.org/10.1101/370940; this version posted July 17, 2018. The copyright holder for this preprint (which was not certified by peer review) is the author/funder, who has granted bioRxiv a license to display the preprint in perpetuity. It is made available under aCC-BY 4.0 International license.

725 **32. Partridge SR, Ginn AN, Paulsen IT, Iredell JR. pEl1573 carrying *bla*$_{IMP-4}$, from**
726 **Sydney, Australia, is closely related to other IncL/M plasmids. Antimicrobial agents**
727 **and chemotherapy. 2012;56(11):6029-32.**

728 **33. Partridge SR, Ginn AN, Wiklendt AM, Ellem J, Wong JS, Ingram P, et al.**
729 **Emergence of *bla*$_{KPC}$ carbapenemase genes in Australia. Int J Antimicrob Agents.**
730 **2015;45(2):130-6.**

731 **34. Zong Z, Partridge SR, Thomas L, Iredell JR. Dominance of *bla*$_{CTX-M}$ within an**
732 **Australian extended-spectrum β-lactamase gene pool. Antimicrobial agents and**
733 **chemotherapy. 2008;52(11):4198-202.**

734 **35. Espedido BA, Partridge SR, Iredell JR. *bla*$_{IMP-4}$ in different genetic contexts in**
735 ***Enterobacteriaceae* isolates from Australia. Antimicrobial agents and chemotherapy.**
736 **2008;52(8):2984-7.**

737 **36. Barton BM, Harding GP, Zuccarelli AJ. A general method for detecting and**
738 **sizing large plasmids. Analytical biochemistry. 1995;226(2):235-40.**

739 **37. Partridge SR, Zong Z, Iredell JR. Recombination in IS*26* and Tn*2* in the**
740 **evolution of multiresistance regions carrying *bla*$_{CTX-M-15}$ on conjugative IncF plasmids**
741 **from *Escherichia coli*. Antimicrobial agents and chemotherapy. 2011;55(11):4971-8.**

bioRxiv preprint doi: https://doi.org/10.1101/370940; this version posted July 17, 2018. The copyright holder for this preprint (which was not certified by peer review) is the author/funder, who has granted bioRxiv a license to display the preprint in perpetuity. It is made available under aCC-BY 4.0 International license.

742 **38. Carlone GM, Thomas ML, Rumschlag HS, Sottnek FO. Rapid microprocedure**
743 **for isolating detergent-insoluble outer membrane proteins from *Haemophilus* species.**
744 **Journal of clinical microbiology. 1986;24(3):330-2.**

745 **39. Rasheed JK, Anderson GJ, Yigit H, Queenan AM, Domenech-Sanchez A,**
746 **Swenson JM, et al. Characterization of the extended-spectrum β-lactamase reference**
747 **strain, *Klebsiella pneumoniae* K6 (ATCC 700603), which produces the novel enzyme**
748 **SHV-18. Antimicrobial agents and chemotherapy. 2000;44(9):2382-8.**

749 **40. Livak KJ, Schmittgen TD. Analysis of relative gene expression data using real-**
750 **time quantitative PCR and the 2(-ΔΔC(T)) Method. Methods. 2001;25(4):402-8.**

751 **41. Knopp M, Andersson DI. Amelioration of the fitness costs of antibiotic resistance**
752 **due to reduced outer membrane permeability by upregulation of alternative porins.**
753 **Molecular biology and evolution. 2015;32(12):3252-63.**

754 **42. Olivares J, Alvarez-Ortega C, Linares JF, Rojo F, Kohler T, Martinez JL.**
755 **Overproduction of the multidrug efflux pump MexEF-OprN does not impair**
756 ***Pseudomonas aeruginosa* fitness in competition tests, but produces specific changes in**
757 **bacterial regulatory networks. Environmental microbiology. 2012;14(8):1968-81.**

758 **43. Nevola JJ, Stocker BA, Laux DC, Cohen PS. Colonization of the mouse intestine**
759 **by an avirulent *Salmonella typhimurium* strain and its lipopolysaccharide-defective**
760 **mutants. Infection and immunity. 1985;50(1):152-9.**

bioRxiv preprint doi: https://doi.org/10.1101/370940; this version posted July 17, 2018. The copyright holder for this preprint (which was not certified by peer review) is the author/funder, who has granted bioRxiv a license to display the preprint in perpetuity. It is made available under aCC-BY 4.0 International license.

761 **44. Favre-Bonte S, Licht TR, Forestier C, Krogfelt KA. *Klebsiella pneumoniae***
762 **capsule expression is necessary for colonization of large intestines of streptomycin-**
763 **treated mice. Infection and immunity. 1999;67(11):6152-6.**

764 **45. Schjorring S, Struve C, Krogfelt KA. Transfer of antimicrobial resistance**
765 **plasmids from *Klebsiella pneumoniae* to *Escherichia coli* in the mouse intestine. The**
766 **Journal of antimicrobial chemotherapy. 2008;62(5):1086-93.**

767 **46. Schjørring S, Struve C, Krogfelt KA. Transfer of antimicrobial resistance**
768 **plasmids from *Klebsiella pneumoniae* to *Escherichia coli* in the mouse intestine. The**
769 **Journal of antimicrobial chemotherapy. 2008;62(5):1086-93.**

770 **47. Chaves J, Ladona MG, Segura C, Coira A, Reig R, Ampurdanes C. SHV-1 beta-**
771 **lactamase is mainly a chromosomally encoded species-specific enzyme in *Klebsiella***
772 ***pneumoniae*. Antimicrobial agents and chemotherapy. 2001;45(10):2856-61.**

773 **48. Haeggman S, Lofdahl S, Paauw A, Verhoef J, Brisse S. Diversity and evolution**
774 **of the class A chromosomal beta-lactamase gene in *Klebsiella pneumoniae*.**
775 **Antimicrobial agents and chemotherapy. 2004;48(7):2400-8.**

776 **49. Bush K, Fisher JF. Epidemiological expansion, structural studies, and clinical**
777 **challenges of new β-lactamases from Gram-negative bacteria. Annual review of**
778 **microbiology. 2011;65:455-78.**

bioRxiv preprint doi: https://doi.org/10.1101/370940; this version posted July 17, 2018. The copyright holder for this preprint (which was not certified by peer review) is the author/funder, who has granted bioRxiv a license to display the preprint in perpetuity. It is made available under aCC-BY 4.0 International license.

779 **50. Tomás JM, Ciurana B, Jofre JT. New, simple medium for selective, differential**
780 **recovery of *Klebsiella spp*. Applied and environmental microbiology. 1986;51(6):1361-3.**

781 **51. Lawlor MS, Hsu J, Rick PD, Miller VL. Identification of *Klebsiella pneumoniae***
782 **virulence determinants using an intranasal infection model. Molecular microbiology.**
783 **2005;58(4):1054-73.**

784 **52. Struve C, Bojer M, Krogfelt KA. Characterization of *Klebsiella pneumoniae* type**
785 **1 fimbriae by detection of phase variation during colonization and infection and impact**
786 **on virulence. Infection and immunity. 2008;76(9):4055-65.**

787 **53. Renois F, Jacques J, Guillard T, Moret H, Pluot M, Andreoletti L, et al.**
788 **Preliminary investigation of a mice model of *Klebsiella pneumoniae subsp. ozaenae***
789 **induced pneumonia. Microbes and infection. 2011;13(12-13):1045-51.**

790 **54. Biasini M, Bienert S, Waterhouse A, Arnold K, Studer G, Schmidt T, et al.**
791 **SWISS-MODEL: modelling protein tertiary and quaternary structure using**
792 **evolutionary information. Nucleic acids research. 2014;42(Web Server issue):W252-8.**

793 **55. Davis IW, Leaver-Fay A, Chen VB, Block JN, Kapral GJ, Wang X, et al.**
794 **MolProbity: all-atom contacts and structure validation for proteins and nucleic acids.**
795 **Nucleic acids research. 2007;35(Web Server issue):W375-83.**

bioRxiv preprint doi: https://doi.org/10.1101/370940; this version posted July 17, 2018. The copyright holder for this preprint (which was not certified by peer review) is the author/funder, who has granted bioRxiv a license to display the preprint in perpetuity. It is made available under aCC-BY 4.0 International license.

796 **56. Chen VB, Arendall WB, 3rd, Headd JJ, Keedy DA, Immormino RM, Kapral GJ,**
797 **et al. MolProbity: all-atom structure validation for macromolecular crystallography.**
798 **Acta crystallographica Section D, Biological crystallography. 2010;66(Pt 1):12-21.**

799 **57. Bowie JU, Luthy R, Eisenberg D. A method to identify protein sequences that**
800 **fold into a known three-dimensional structure. Science. 1991;253(5016):164-70.**

801 **58. Luthy R, Bowie JU, Eisenberg D. Assessment of protein models with three-**
802 **dimensional profiles. Nature. 1992;356(6364):83-5.**

803 **59. Schrodinger L. The PyMOL Molecular Graphics System, Version 2.1.1. 2015.**

804 **60. Lee RS, Seemann T, Heffernan H, Kwong JC, Goncalves da Silva A, Carter GP,**
805 **et al. Genomic epidemiology and antimicrobial resistance of *Neisseria gonorrhoeae* in**
806 **New Zealand. The Journal of antimicrobial chemotherapy. 2018;73(2):353-64.**

807 **61. Bankevich A, Nurk S, Antipov D, Gurevich AA, Dvorkin M, Kulikov AS, et al.**
808 **SPAdes: a new genome assembly algorithm and its applications to single-cell**
809 **sequencing. J Comput Biol. 2012;19(5):455-77.**

810 **62. Darling AE, Mau B, Perna NT. progressiveMauve: multiple genome alignment**
811 **with gene gain, loss and rearrangement. PloS one. 2010;5(6):e11147.**

812 **63. Seemann T. Prokka: rapid prokaryotic genome annotation. Bioinformatics.**
813 **2014;30(14):2068-9.**

bioRxiv preprint doi: https://doi.org/10.1101/370940; this version posted July 17, 2018. The copyright holder for this preprint (which was not certified by peer review) is the author/funder, who has granted bioRxiv a license to display the preprint in perpetuity. It is made available under aCC-BY 4.0 International license.

814 **64. Lam MMC, Wick RR, Wyres KL, Gorrie C, Judd LM, Brisse S, et al. Frequent**
815 **emergence of pathogenic lineages of *Klebsiella pneumoniae* via mobilisation of**
816 **yersiniabactin and colibactin. bioRxiv. 2017.**

817 **65. Page AJ, Cummins CA, Hunt M, Wong VK, Reuter S, Holden MT, et al. Roary:**
818 **rapid large-scale prokaryote pan genome analysis. Bioinformatics. 2015;31(22):3691-3.**

819 **66. Nguyen LT, Schmidt HA, von Haeseler A, Minh BQ. IQ-TREE: a fast and**
820 **effective stochastic algorithm for estimating maximum-likelihood phylogenies.**
821 **Molecular biology and evolution. 2015;32(1):268-74.**

822 **67. Hadfield J, Croucher NJ, Goater RJ, Abudahab K, Aanensen DM, Harris SR.**
823 **Phandango: an interactive viewer for bacterial population genomics. Bioinformatics.**
824 **2017.**

825 **68. Haanperä M, Forssten SD, Huovinen P, Jalava J. Typing of SHV extended-**
826 **spectrum β-lactamases by pyrosequencing in *Klebsiella pneumoniae* strains with**
827 **chromosomal SHV β-lactamase. Antimicrobial agents and chemotherapy.**
828 **2008;52(7):2632-5.**

829 **69. Babini GS, Livermore DM. Are SHV β-lactamases universal in *Klebsiella***
830 ***pneumoniae*? Antimicrobial agents and chemotherapy. 2000;44(8):2230.**

bioRxiv preprint doi: https://doi.org/10.1101/370940; this version posted July 17, 2018. The copyright holder for this preprint (which was not certified by peer review) is the author/funder, who has granted bioRxiv a license to display the preprint in perpetuity. It is made available under aCC-BY 4.0 International license.

831 **70. Hæggman S, Löfdahl S, Paauw A, Verhoef J, Brisse S. Diversity and evolution of**
832 **the class A chromosomal β-lactamase gene in *Klebsiella pneumoniae*. Antimicrobial**
833 **agents and chemotherapy. 2004;48(7):2400-8.**

834 **71. Chaves J, Ladona MG, Segura C, Coira A, Reig R, Ampurdanés C. SHV-1 β-**
835 **lactamase is mainly a chromosomally encoded species-specific enzyme in *Klebsiella***
836 ***pneumoniae*. Antimicrobial agents and chemotherapy. 2001;45(10):2856-61.**

837 **72. EUCAST. The European Committee on Antimicrobial Susceptibility Testing.**
838 **Breakpoint tables for interpretation of MICs and zone diameters. Version 8.0.**
839 **www.eucast.org: European Committee on Antimicrobial Susceptibility Testing; 2018.**

840 **73. CLSI. M100-S24. *Performance Standards for Antimicrobial Susceptibility Testing;***
841 ***Twenty-Fourth Informational Supplement.* Clinical and Laboratory Standards Institute;**
842 **Wayne, PA. 2014.**

843 **74. Garcia-Sureda L, Juan C, Domenech-Sanchez A, Alberti S. Role of *Klebsiella***
844 ***pneumoniae* LamB Porin in antimicrobial resistance. Antimicrobial agents and**
845 **chemotherapy. 2011;55(4):1803-5.**

846 **75. Kaczmarek FM, Dib-Hajj F, Shang W, Gootz TD. High-level carbapenem**
847 **resistance in a *Klebsiella pneumoniae* clinical isolate is due to the combination of bla_{ACT-1}**
848 **β-lactamase production, porin OmpK35/36 insertional inactivation, and down-**
849 **regulation of the phosphate transport porin PhoE. Antimicrobial agents and**
850 **chemotherapy. 2006;50(10):3396-406.**

bioRxiv preprint doi: https://doi.org/10.1101/370940; this version posted July 17, 2018. The copyright holder for this preprint (which was not certified by peer review) is the author/funder, who has granted bioRxiv a license to display the preprint in perpetuity. It is made available under aCC-BY 4.0 International license.

851 **76. Doménech-Sánchez A, Martínez-Martínez L, Hernández-Allés S, del Carmen**
852 **Conejo M, Pascual A, Tomás JM, et al. Role of *Klebsiella pneumoniae* OmpK35 porin in**
853 **antimicrobial resistance. Antimicrobial agents and chemotherapy. 2003;47(10):3332-5.**

854 **77. Garcia-Sureda L, Domenech-Sanchez A, Barbier M, Juan C, Gasco J, Alberti S.**
855 **OmpK26, a novel porin associated with carbapenem resistance in *Klebsiella***
856 ***pneumoniae*. Antimicrobial agents and chemotherapy. 2011;55(10):4742-7.**

857 **78. Tsai YK, Fung CP, Lin JC, Chen JH, Chang FY, Chen TL, et al. *Klebsiella***
858 ***pneumoniae* outer membrane porins OmpK35 and OmpK36 play roles in both**
859 **antimicrobial resistance and virulence. Antimicrobial agents and chemotherapy.**
860 **2011;55(4):1485-93.**

861 **79. March C, Cano V, Moranta D, Llobet E, Perez-Gutierrez C, Tomas JM, et al.**
862 **Role of bacterial surface structures on the interaction of *Klebsiella pneumoniae* with**
863 **phagocytes. PloS one. 2013;8(2):e56847.**

864 **80. Pitout JD, Sanders CC, Sanders WE, Jr. Antimicrobial resistance with focus on**
865 **β-lactam resistance in Gram-negative bacilli. Am J Med. 1997;103(1):51-9.**

866 **81. Fridkin SK, Steward CD, Edwards JR, Pryor ER, McGowan JE, Jr., Archibald**
867 **LK, et al. Surveillance of antimicrobial use and antimicrobial resistance in United**
868 **States hospitals: project ICARE phase 2. Project Intensive Care Antimicrobial**
869 **Resistance Epidemiology (ICARE) hospitals. Clinical infectious diseases : an official**
870 **publication of the Infectious Diseases Society of America. 1999;29(2):245-52.**

bioRxiv preprint doi: https://doi.org/10.1101/370940; this version posted July 17, 2018. The copyright holder for this preprint (which was not certified by peer review) is the author/funder, who has granted bioRxiv a license to display the preprint in perpetuity. It is made available under aCC-BY 4.0 International license.

871 **82. Hidron AI, Edwards JR, Patel J, Horan TC, Sievert DM, Pollock DA, et al.**
872 **NHSN annual update: antimicrobial-resistant pathogens associated with healthcare-**
873 **associated infections: annual summary of data reported to the National Healthcare**
874 **Safety Network at the Centers for Disease Control and Prevention, 2006-2007. Infection**
875 **control and hospital epidemiology : the official journal of the Society of Hospital**
876 **Epidemiologists of America. 2008;29(11):996-1011.**

877 **83. Wollheim C, Guerra IM, Conte VD, Hoffman SP, Schreiner FJ, Delamare AP, et**
878 **al. Nosocomial and community infections due to class A extended-spectrum beta-**
879 **lactamase (ESBLA)-producing *Escherichia coli* and *Klebsiella spp*. in southern Brazil.**
880 **The Brazilian journal of infectious diseases : an official publication of the Brazilian**
881 **Society of Infectious Diseases. 2011;15(2):138-43.**

882 **84. Doumith M, Ellington MJ, Livermore DM, Woodford N. Molecular mechanisms**
883 **disrupting porin expression in ertapenem-resistant *Klebsiella* and *Enterobacter* spp.**
884 **clinical isolates from the UK. The Journal of antimicrobial chemotherapy.**
885 **2009;63(4):659-67.**

886 **85. Chudácková E, Bergerová T, Fajfrlík K, Cervená D, Urbásková P, Empel J, et**
887 **al. Carbapenem-nonsusceptible strains of *Klebsiella pneumoniae* producing SHV-5**
888 **and/or DHA-1 β-lactamases in a Czech hospital. FEMS microbiology letters.**
889 **2010;309(1):62-70.**

bioRxiv preprint doi: https://doi.org/10.1101/370940; this version posted July 17, 2018. The copyright holder for this preprint (which was not certified by peer review) is the author/funder, who has granted bioRxiv a license to display the preprint in perpetuity. It is made available under aCC-BY 4.0 International license.

890 **86. Nikaido H, Rosenberg EY. Effect on solute size on diffusion rates through the**
891 **transmembrane pores of the outer membrane of *Escherichia coli*. J Gen Physiol.**
892 **1981;77(2):121-35.**

893 **87. Jaffe A, Chabbert YA, Semonin O. Role of porin proteins OmpF and OmpC in**
894 **the permeation of β-lactams. Antimicrobial agents and chemotherapy. 1982;22(6):942-8.**

895 **88. Nitzan Y, Deutsch EB, Pechatnikov I. Diffusion of β-lactam antibiotics through**
896 **oligomeric or monomeric porin channels of some Gram-negative bacteria. Curr**
897 **Microbiol. 2002;45(6):446-55.**

898 **89. Sugawara E, Kojima S, Nikaido H. *Klebsiella pneumoniae* major porins OmpK35**
899 **and OmpK36 allow more efficient diffusion of β-lactams than their *Escherichia coli***
900 **homologs OmpF and OmpC. Journal of bacteriology. 2016;198(23):3200-8.**

901 **90. Chen JH, Siu LK, Fung CP, Lin JC, Yeh KM, Chen TL, et al. Contribution of**
902 **outer membrane protein K36 to antimicrobial resistance and virulence in *Klebsiella***
903 ***pneumoniae*. The Journal of antimicrobial chemotherapy. 2010;65(5):986-90.**

904 **91. Tsai YK, Liou CH, Fung CP, Lin JC, Siu LK. Single or in combination**
905 **antimicrobial resistance mechanisms of *Klebsiella pneumoniae* contribute to varied**
906 **susceptibility to different carbapenems. PloS one. 2013;8(11):e79640.**

bioRxiv preprint doi: https://doi.org/10.1101/370940; this version posted July 17, 2018. The copyright holder for this preprint (which was not certified by peer review) is the author/funder, who has granted bioRxiv a license to display the preprint in perpetuity. It is made available under aCC-BY 4.0 International license.

907 **92. Bedikian A, Okamoto MP, Nakahiro RK, Farino J, Heseltine PN, Appleman**
908 **MD, et al. Pharmacokinetics of meropenem in patients with intra-abdominal infections.**
909 **Antimicrobial agents and chemotherapy. 1994;38(1):151-4.**

910 **93. Condon RE, Walker AP, Hanna CB, Greenberg RN, Broom A, Pitkin D.**
911 **Penetration of meropenem in plasma and abdominal tissues from patients undergoing**
912 **intraabdominal surgery. Clinical infectious diseases : an official publication of the**
913 **Infectious Diseases Society of America. 1997;24 Suppl 2:S181-3.**

914 **94. Hughes D, Andersson DI. Evolutionary consequences of drug resistance: shared**
915 **principles across diverse targets and organisms. Nature reviews Genetics.**
916 **2015;16(8):459-71.**

917 **95. Kaczmarek FM, Dib-Hajj F, Shang W, Gootz TD. High-level carbapenem**
918 **resistance in a *Klebsiella pneumoniae* clinical isolate is due to the combination of bla_{ACT-1}**
919 **β-lactamase production, porin OmpK35/36 insertional inactivation, and down-**
920 **regulation of the phosphate transport porin *phoE*. Antimicrobial agents and**
921 **chemotherapy. 2006;50(10):3396-406.**

922 **96. Wise MG, Horvath E, Young K, Sahm DF, Kazmierczak KM. Global survey of**
923 ***Klebsiella pneumoniae* major porins from ertapenem non-susceptible isolates lacking**
924 **carbapenemases. Journal of medical microbiology. 2018;67(3):289-95.**

bioRxiv preprint doi: https://doi.org/10.1101/370940; this version posted July 17, 2018. The copyright holder for this preprint (which was not certified by peer review) is the author/funder, who has granted bioRxiv a license to display the preprint in perpetuity. It is made available under aCC-BY 4.0 International license.

925 **97. De E, Baslé A, Jaquinod M, Saint N, Malléa M, Molle G, et al. A new mechanism**
926 **of antibiotic resistance in *Enterobacteriaceae* induced by a structural modification of the**
927 **major porin. Molecular microbiology. 2001;41(1):189-98.**

928 **98. Olesky M, Zhao S, Rosenberg RL, Nicholas RA. Porin-mediated antibiotic**
929 **resistance in *Neisseria gonorrhoeae*: ion, solute, and antibiotic permeation through PIB**
930 **proteins with penB mutations. Journal of bacteriology. 2006;188(7):2300-8.**

931 **99. Lou H, Chen M, Black SS, Bushell SR, Ceccarelli M, Mach T, et al. Altered**
932 **antibiotic transport in OmpC mutants isolated from a series of clinical strains of multi-**
933 **drug resistant *E. coli*. PloS one. 2011;6(10):e25825.**

934 **100. Bredin J, Saint N, Mallea M, De E, Molle G, Pagès JM, et al. Alteration of pore**
935 **properties of *Escherichia coli* OmpF induced by mutation of key residues in anti-loop 3**
936 **region. Biochem J. 2002;363(Pt 3):521-8.**

937 **101. Thiolas A, Bornet C, Davin-Regli A, Pagès JM, Bollet C. Resistance to imipenem,**
938 **cefepime, and cefpirome associated with mutation in Omp36 osmoporin of *Enterobacter***
939 ***aerogenes*. Biochem Biophys Res Commun. 2004;317(3):851-6.**

940 **102. Sugawara E, Kojima S, Nikaido H. *Klebsiella pneumoniae* major porins OmpK35**
941 **and OmpK36 allow more efficient diffusion of β-Lactams than their *Escherichia coli***
942 **homologs OmpF and OmpC. Journal of bacteriology. 2016;198(23):3200-8.**

bioRxiv preprint doi: https://doi.org/10.1101/370940; this version posted July 17, 2018. The copyright holder for this preprint (which was not certified by peer review) is the author/funder, who has granted bioRxiv a license to display the preprint in perpetuity. It is made available under aCC-BY 4.0 International license.

943 **103. Bornet C, Saint N, Fetnaci L, Dupont M, Davin-Regli A, Bollet C, et al. Omp35,**
944 **a new *Enterobacter aerogenes* porin involved in selective susceptibility to**
945 **cephalosporins. Antimicrobial agents and chemotherapy. 2004;48(6):2153-8.**

946 **104. Woodford N, Turton JF, Livermore DM. Multiresistant Gram-negative bacteria:**
947 **the role of high-risk clones in the dissemination of antibiotic resistance. FEMS**
948 **microbiology reviews. 2011;35(5):736-55.**

949 **105. Wright LL, Turton JF, Livermore DM, Hopkins KL, Woodford N. Dominance**
950 **of international 'high-risk clones' among metallo-beta-lactamase-producing**
951 ***Pseudomonas aeruginosa* in the UK. The Journal of antimicrobial chemotherapy.**
952 **2015;70(1):103-10.**

953 **106. Andersson DI, Hughes D. Microbiological effects of sublethal levels of**
954 **antibiotics. Nature reviews Microbiology. 2014;12(7):465-78.**

955 **107. Yang Y, Song W, Lin H, Wang W, Du L, Xing W. Antibiotics and antibiotic**
956 **resistance genes in global lakes: A review and meta-analysis. Environment**
957 **international. 2018;116:60-73.**

958 **108. Pulzova L, Navratilova L, Comor L. Alterations in outer membrane**
959 **permeability favor drug-resistant phenotype of *Klebsiella pneumoniae*. Microbial drug**
960 **resistance. 2017;23(4):413-20.**

bioRxiv preprint doi: https://doi.org/10.1101/370940; this version posted July 17, 2018. The copyright holder for this preprint (which was not certified by peer review) is the author/funder, who has granted bioRxiv a license to display the preprint in perpetuity. It is made available under aCC-BY 4.0 International license.

961 **109. Elena SF, Lenski RE. Evolution experiments with microorganisms: the dynamics**
962 **and genetic bases of adaptation. Nature reviews Genetics. 2003;4(6):457-69.**

963 **110. Harder KJ, Nikaido H, Matsuhashi M. Mutants of *Escherichia coli* that are**
964 **resistant to certain beta-lactam compounds lack the *ompF* porin. Antimicrobial agents**
965 **and chemotherapy. 1981;20(4):549-52.**

966 **111. Hasegawa Y, Yamada H, Mizushima S. Interactions of outer membrane proteins**
967 **O-8 and O-9 with peptidoglycan sacculus of *Escherichia coli* K-12. Journal of**
968 **biochemistry. 1976;80(6):1401-9.**

969 **112. Matsubara M, Kitaoka SI, Takeda SI, Mizuno T. Tuning of the porin expression**
970 **under anaerobic growth conditions by his-to-Asp cross-phosphorelay through both the**
971 **EnvZ-osmosensor and ArcB-anaerosensor in *Escherichia coli*. Genes to cells : devoted**
972 **to molecular & cellular mechanisms. 2000;5(7):555-69.**

973 **113. Heyde M, Portalier R. Regulation of major outer membrane porin proteins of**
974 ***Escherichia coli* K 12 by pH. Molecular & general genetics : MGG. 1987;208(3):511-7.**

975 **114. Giraud A, Arous S, De Paepe M, Gaboriau-Routhiau V, Bambou JC, Rakotobe**
976 **S, et al. Dissecting the genetic components of adaptation of *Escherichia coli* to the mouse**
977 **gut. PLoS genetics. 2008;4(1):e2.**

978

bioRxiv preprint doi: https://doi.org/10.1101/370940; this version posted July 17, 2018. The copyright holder for this preprint (which was not certified by peer review) is the author/funder, who has granted bioRxiv a license to display the preprint in perpetuity. It is made available under aCC-BY 4.0 International license.

Supplemental information

Figure S1: S1/PFGE of strains with the conjugated plasmids. White arrows show the plasmids in original host isolates and transconjugants. MW; Mid-range PFG Marker**.**

Figure S2: *In vitro* and *in vivo* competition experiments in *K. pneumoniae* ATCC 13883, 10.85 and 11.76 knock-out porin mutants. The relative fitness of deletion porin mutants in comparison with parental strain (ATCC 13883, 10.85 or 11.76) was performed by competition experiments in co-cultures and expressed as a percentage of the mutant or wild type cells versus total population at each time point. *In vitro* growth conditions, MH broth, 37ºC. Panels 1, 3 and 4 represent *in vitro* competition experiments for ATCC 13383, 10.85 and 11.76, respectively. Panels in row 2 show *in vivo* competition experiments for ATCC 13383. For *in vivo* competition experiments, the values for each mouse are represented individually. Violet diamond, ATCC 13883, 10.85 or 11.76 wild type strains. Orange square, ΔOmpK35 mutant. Red square, ΔOmpK36 mutant. Blue circle, ΔOmpK35ΔOmpK36 mutant.

Figure S3: Individual gut colonization. *K. pneumoniae* intestinal colonization in a mouse model. CFU counts of *K. pneumoniae* ATCC 13883 and porin mutants from mice faecal sample. Bacterial inoculum at day 0 is 1x1010 CFU /mouse. Addition of ampicillin 0.5 g / L in the drinking water on day 4. Violet diamond, ATCC 13883 wild type strains. Orange square, ΔOmpK35 mutant. Red square, ΔOmpK36 mutant. Blue circle, ΔOmpK35ΔOmpK36 mutant. Green square, OmpK36GD mutant. Pink circle, ΔOmpK35OmpK36GD mutant.

Fig S4: Alignment of *Klebsiella pneumoniae* OmpK36 proteins. 26 unique sequences with OmpK36 L3 variants from GenBank were compared with OmpK36 of NTUH_K2044. Isolates with wild-type L3 sequence are not included. Dot line, signal peptide. Black line, beta strands. Red line, loops. Blue line, alpha helix. Green squares, turns. OmpK36 secondary

bioRxiv preprint doi: https://doi.org/10.1101/370940; this version posted July 17, 2018. The copyright holder for this preprint (which was not certified by peer review) is the author/funder, who has granted bioRxiv a license to display the preprint in perpetuity. It is made available under aCC-BY 4.0 International license.

1002 structure based on previous studies. (1, 2). Red boxes, residues involved in the pore eyelet
1003 based on (3). Black box, L3 variants.

1004 1. Cowan SW, Schirmer T, Rummel G, Steiert M, Ghosh R, Pauptit RA, et al. Crystal
1005 structures explain functional properties of two *E. coli* porins. Nature. 1992;358(6389):727-33.

1006 2. Domenech-Sanchez A, Hernandez-Alles S, Martinez-Martinez L, Benedi VJ,
1007 Alberti S. Identification and characterization of a new porin gene of *Klebsiella pneumoniae*:
1008 its role in β-lactam antibiotic resistance. J Bacteriol. 1999;181(9):2726-32.

1009 3. Bornet C, Saint N, Fetnaci L, Dupont M, Davin-Regli A, Bollet C, et al. Omp35, a
1010 new Enterobacter aerogenes porin involved in selective susceptibility to cephalosporins.
1011 Antimicrob Agents Chemother. 2004;48(6):2153-8.

1012 **Figure S5: Proposed scenario of the major duplications observed in OmpK36 loop 3.**
1013 Based on observations of the codon sequences, the extra –SD and –SYG following GGD
1014 likely result from a combination of duplication followed by point mutation.

1015 **Figure S6: Phylogenetic tree of an Australian collection of *K. pneumoniae* isolates with**
1016 **various degrees of non-susceptibility to carbapanems.** Metadata includes year of isolation;
1017 MIC levels for ETP: ertapenem, IMP: imipenem, and MEM: meropenem; *ompK36* L3
1018 mutation; *ompK35* disrupted mutations (as listed in Table S7); ST: sequence type; number of
1019 predicted resistance genes encoded; carbapenamase gene encoded; ESBL: extended-spectrum
1020 beta-lactamase gene encoded.

bioRxiv preprint doi: https://doi.org/10.1101/370940; this version posted July 17, 2018. The copyright holder for this preprint (which was not certified by peer review) is the author/funder, who has granted bioRxiv a license to display the preprint in perpetuity. It is made available under aCC-BY 4.0 International license.

Figure S7: Imbalanced features of the 1,557 *Klebsiella pneumoniae* genomes found in Genbank (February 2017). Bubble chart showing the distribution of isolates across countries with at least 2 *Klebsiella pneumoniae* genomes reported, from 2001 to 2016, and coloured according to their MLST. The size of each circle is proportional to the number of isolates.

Figure S8: Extended mosaic plot of the observed proportions of isolates with porins OmpK35 and OmpK36 variations, across STs harbouring *ompK36* GD/TD variants. The mosaic plot shows the relationships between 3 variables; ST (in purple) and presence/absence of *ompK35* (in black) on the *x*-axis; and presence/absence and mutations of *ompK36* (in grey) on the *y*-axis. The size of each plot tile is proportional to counts. Plot tiles are colored according to their standardized Pearson residuals, as determined by a log-linear model. Deeper shades of red and blue corresponding to a standardized residual less than -4 or greater than +4, respectively, can be interpreted as combinations observed significantly less or more than expected (under the assumptions that proportions have equal levels).

Figure S9: Extended mosaic plot of the observed proportions of isolates with porins OmpK35 and OmpK36 variations versus years. The mosaic plots show the relationships between 2 variables; A) year of isolation on the *x*-axis and presence/absence of *ompK35* on the *y*-axis; B) year of isolation on the *x*-axis, and presence/absence and mutations of *ompK36* on the *y*-axis. The size of each plot tile is proportional to counts. Plot tiles are colored according to their standardized Pearson residuals, as determined by a log-linear model. Deeper shades of red and blue corresponding to a standardized residual less than -4 or greater than +4, respectively, can be interpreted as combinations observed significantly less or more than expected (under the assumptions that proportions have equal levels).

Figure S10: Extended mosaic plot of the observed proportions of isolates with porins OmpK35 and OmpK36 variations versus countries. The mosaic plots show the relationships between 2 variables; A) country of isolation on the *x*-axis and presence/absence

bioRxiv preprint doi: https://doi.org/10.1101/370940; this version posted July 17, 2018. The copyright holder for this preprint (which was not certified by peer review) is the author/funder, who has granted bioRxiv a license to display the preprint in perpetuity. It is made available under aCC-BY 4.0 International license.

of *ompK35* on the *y*-axis; B) country of isolation on the *x*-axis, and presence/absence and mutations of *ompK36* on the *y*-axis. The size of each plot tile is proportional to counts. Plot tiles are colored according to their standardized Pearson residuals, as determined by a log-linear model. Deeper shades of red and blue corresponding to a standardized residual less than -4 or greater than +4, respectively, can be interpreted as combinations observed significantly less or more than expected (under the assumptions that proportions have equal levels).

Figure S11: Distribution of resistance genes identified in ST harbouring OmpK36GD or OmpK36TD mutants. Boxplots were used to display the distribution of resistance genes identified with Abricate within each ST with the following OmpK36 variants, namely isolates with –GD in bright red, –TD in brown, or no insertion (–) in grey. Mean comparison *p*-values are also shown for each ST (Wilcoxon test, with '-' used as a reference group; ns: $p > 0.05$; *: $p <= 0.05$; **: $p <= 0.01$; ***: $p <= 0.001$; ****: $p <= 0.0001$). In addition, the corresponding underlying isolate population is also visualised as individual points, coloured according to OmpK35 type, (1) intact in turquoise or (0) disrupted in coral.

Figure S12: SDS-PAGE analysis of outer membrane porins. Wild type strains ATCC 13883, 10.85 and 11.76 were cultured under different temperatures (37^{o}C, 30^{o}C and 25^{o}C) and different nutrient concentrations (MH and MH 1:10). Blue arrow, OmpK35. Black arrow, OmpK36. Red arrow, OmpA.

Figure S13: *In vitro* competition experiments in MH 1:10 dilution. The relative fitness of porin mutants in comparison with parental strain ATCC 13883 was performed by competition experiments in co-cultures and expressed as a percentage of the mutant or wild type cells versus total population at each time point. *In vitro* growth conditions: A, MH 1:10 broth,

bioRxiv preprint doi: https://doi.org/10.1101/370940; this version posted July 17, 2018. The copyright holder for this preprint (which was not certified by peer review) is the author/funder, who has granted bioRxiv a license to display the preprint in perpetuity. It is made available under aCC-BY 4.0 International license.

25°C; B, MH 1:10 broth, 37°C. Violet diamond, ATCC 13883. Orange square, ΔOmpK35. Red square, ΔOmpK36.

Figure S14: Distinct channel restrictions of OmpK36 di-nucleotide mutants (–GD, –TD, and –SD). Comparison of the reference OmpK36 structure under PDB accession 5nup1A (WT, wild type) against predicted structural models of mutants harbouring a di-nucleotide insertion in loop 3 after G113, namely GGDGD, GGDTD and GGDSD. For each predicted structure, the 2 most protruding amino-acids resulting from the di-nucleotide insertion were marked and coloured according to their backbone structure (carbons in yellow, oxygens in red and nitrogens in blue).

Figure S15: **A. Alignment of *E. coli* OmpC_L3 variants**. 11 unique Omp36_L3 variants from GenBank were compared with L3 of OmpC of K-12 MG1655 (NP_416719). Black boxes, residues different from NP_416719. **B. Alignment of *E. aerogenes* Omp36_L3 variants**. Four unique Omp36_L3 variants from GenBank were compared with L3 of Omp36 from ATCC 13048 (AF335467). Black boxes, residues different from AF335467.

Isolates with wild-type L3 sequence are not included. Black line, loop 3. OmpK36 L3 location based on previous studies. (1, 2). Red boxes, residues involved in the pore eyelet based on (3).

1. Cowan SW, Schirmer T, Rummel G, Steiert M, Ghosh R, Pauptit RA, et al. Crystal structures explain functional properties of two *E. coli* porins. Nature. 1992;358(6389):727-33.

2. Domenech-Sanchez A, Hernandez-Alles S, Martinez-Martinez L, Benedi VJ, Alberti S. Identification and characterization of a new porin gene of *Klebsiella pneumoniae*: its role in β-lactam antibiotic resistance. J Bacteriol. 1999;181(9):2726-32.

bioRxiv preprint doi: https://doi.org/10.1101/370940; this version posted July 17, 2018. The copyright holder for this preprint (which was not certified by peer review) is the author/funder, who has granted bioRxiv a license to display the preprint in perpetuity. It is made available under aCC-BY 4.0 International license.

1091 3. Bornet C, Saint N, Fetnaci L, Dupont M, Davin-Regli A, Bollet C, et al. Omp35, a new
1092 Enterobacter aerogenes porin involved in selective susceptibility to cephalosporins.
1093 Antimicrob Agents Chemother. 2004;48(6):2153-8.

1094

1095 **Table S1: Primers and plasmids used during this work**.

1096 **Table S2: Genbank metadata.**

1097 **Table S3: Resistance and typing screening.**

1098 **Table S4: Antibiotic MICs against *K. pneumoniae* and porin mutants.**

1099 **Table S5: Real-time RT-PCR in *K. pneumoniae* ATCC 13883 and 10.85 porin mutants.**
1100 The expression of *rpoD* was used to normalize the results. The levels of expression of each
1101 mutant are shown relative to the wild type strain ATCC 13883 or 10.85.

1102 **Table S6: Relative growth rate and doubling time of *K. pneumoniae* and porin mutants.**

1103 **Table S7: Model evaluation results ATCC 13883 OmpK36 L3variants.**

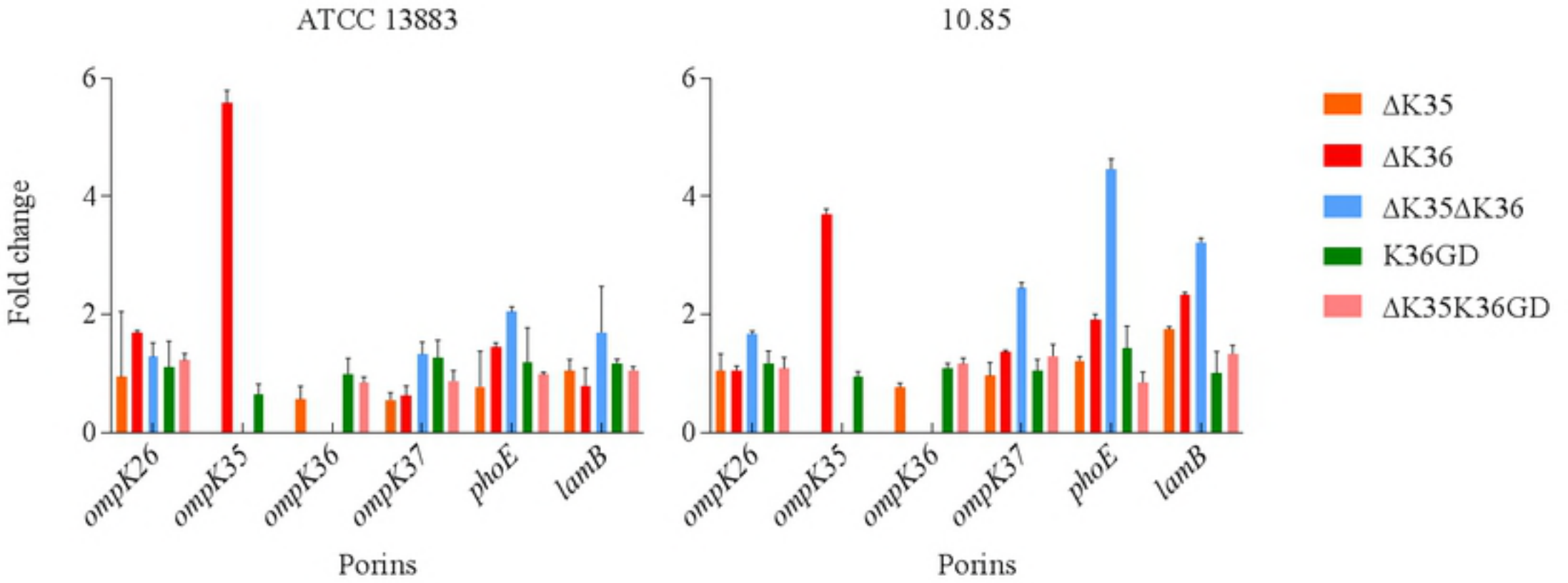
ATCC 13883
10.85
Fold change
0
2
4
6
ompK26
ompK35
ompK36
ompK37
phoE
lamB
Porins
ΔK35
ΔK36
ΔK35ΔK36
K36GD
ΔK35K36GD

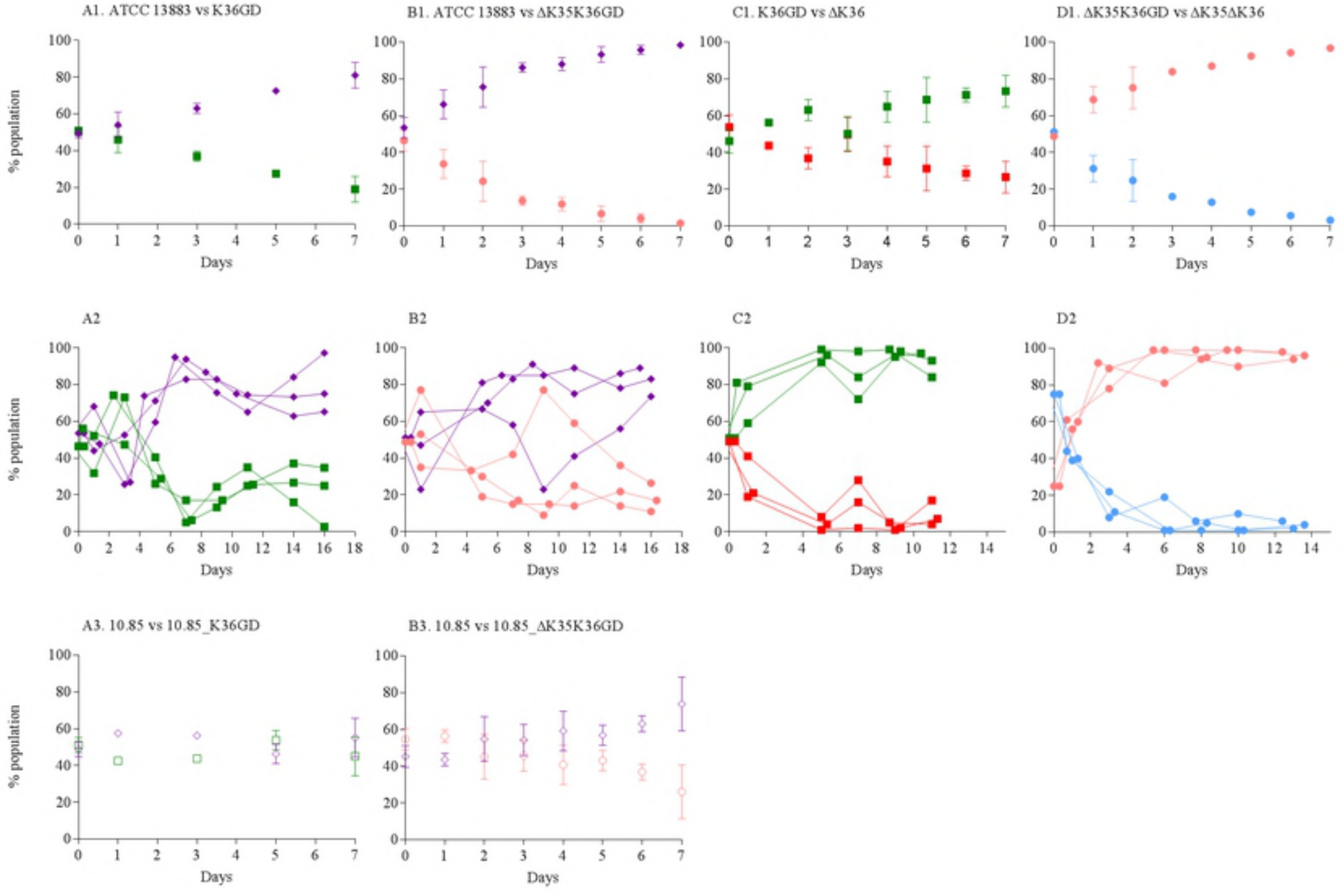
A1. ATCC 13883 vs K36GD
B1. ATCC 13883 vs ΔK35K36GD
C1. K36GD vs ΔK36
D1. ΔK35K36GD vs ΔK35ΔK36
A2
B2
C2
D2
A3. 10.85 vs 10.85_K36GD
B3. 10.85 vs 10.85_ΔK35K36GD
% population
Days

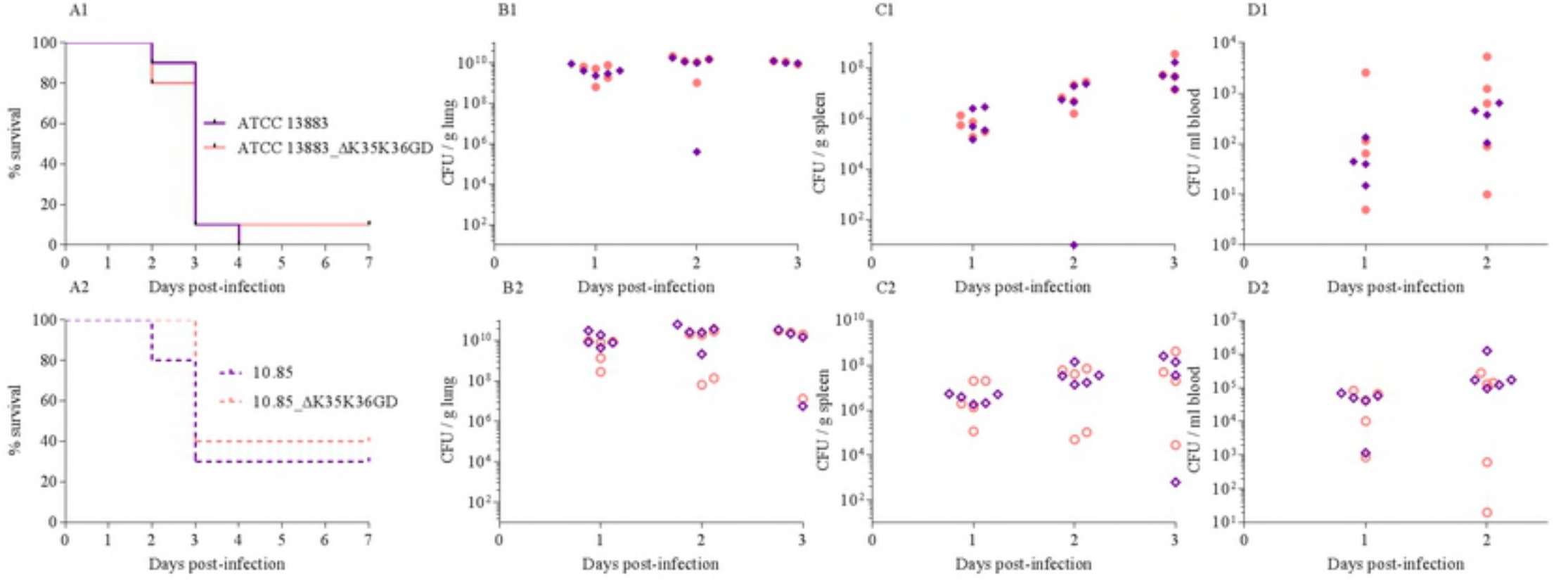
A1
% survival
ATCC 13883
ATCC 13883_ΔK35K36GD
Days post-infection
B1
CFU / g lung
Days post-infection
C1
CFU / g spleen
Days post-infection
D1
CFU / ml blood
Days post-infection
A2
% survival
10.85
10.85_ΔK35K36GD
Days post-infection
B2
CFU / g lung
Days post-infection
C2
CFU / g spleen
Days post-infection
D2
CFU / ml blood
Days post-infection

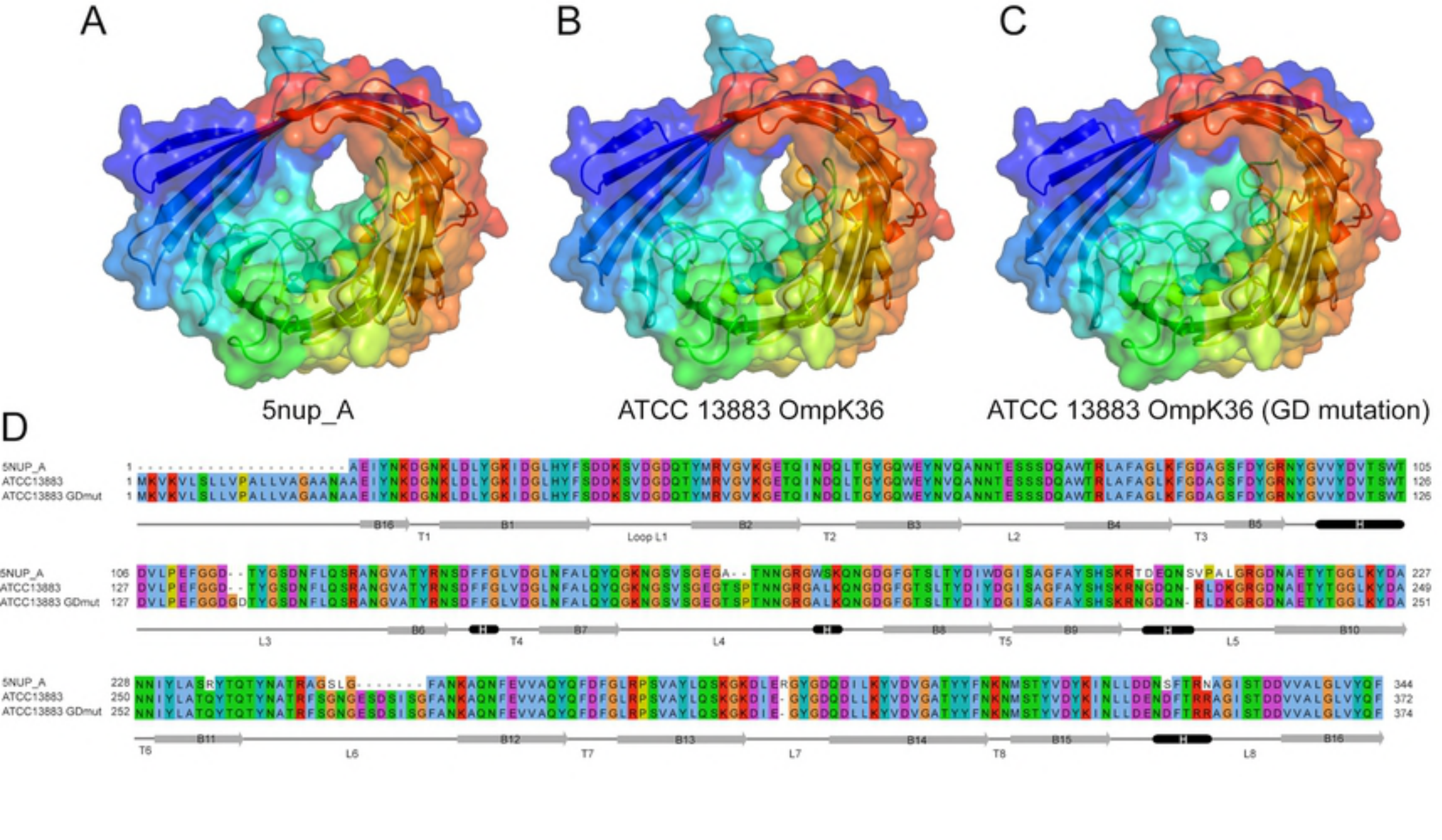
A
B
C
5nup_A
ATCC 13883 OmpK36
ATCC 13883 OmpK36 (GD mutation)
D
5NUP_A
ATCC13883
ATCC13883 GDmut
B16
T1
B1
Loop L1
B2
T2
B3
L2
B4
T3
B5
L3
B6
T4
B7
L4
B8
T5
B9
L5
B10
T6
B11
L6
B12
T7
B13
L7
B14
T8
B15
L8
B16

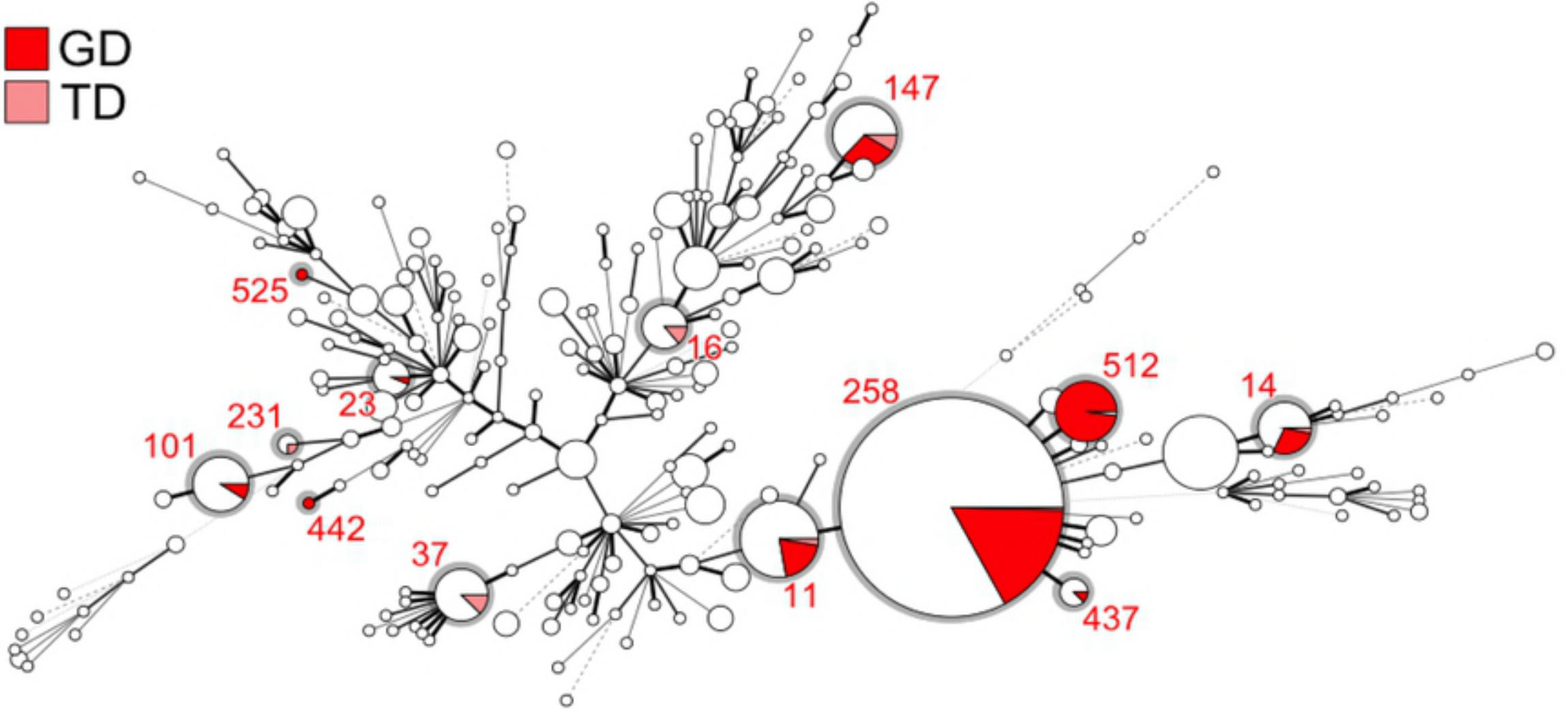
GD
TD
147
525
16
512
14
258
23
231
101
442
37
11
437

available under aCC-BY 4.0 International license.